CHAPTER III

AN INCOMMENSURATE SMECTIC A PHASE

3.1 INTRODUCTION

The smectic A phase is characterized by a layered arrangement of rod-like molecules,[1] the long axis of the molecule being referred to as the director ($\vec{n}$). The average orientation of the long axis of the molecules is normal to the layers. The X-ray diffraction pattern of an unaligned smectic A phase shows a sharp low angle ring (Bragg angle $\theta \sim 1°$) corresponding to the smectic layer thickness and a large angle diffuse ring ($\theta \sim 10°$) corresponding to the inter-molecular distance within a layer.[2] The diffuse nature of the outer ring shows that the in-plane correlations within a layer are liquid-like.

Perhaps a more realistic representation of the smectic A phase is to describe it as an orientationally ordered fluid with a one-dimensional[3,4] mass-density wave along the optic axis (see Fig. 3.1). This mass density wave along the Z-axis, i.e., along the director is well described[3] by

$$\rho(r) = \rho_0 [1 + \mathrm{Re}\{|\psi| \exp i (q_0 Z + \phi)\}] ,$$

where $q_0 = 2\pi/d$ is the wavevector at which the X-ray diffraction peak corresponding to the layer spacing (d) occurs in reciprocal space, ϕ is a phase factor which fixes the position of the layers, $|\psi|$ is the amplitude of the density wave which is a measure of

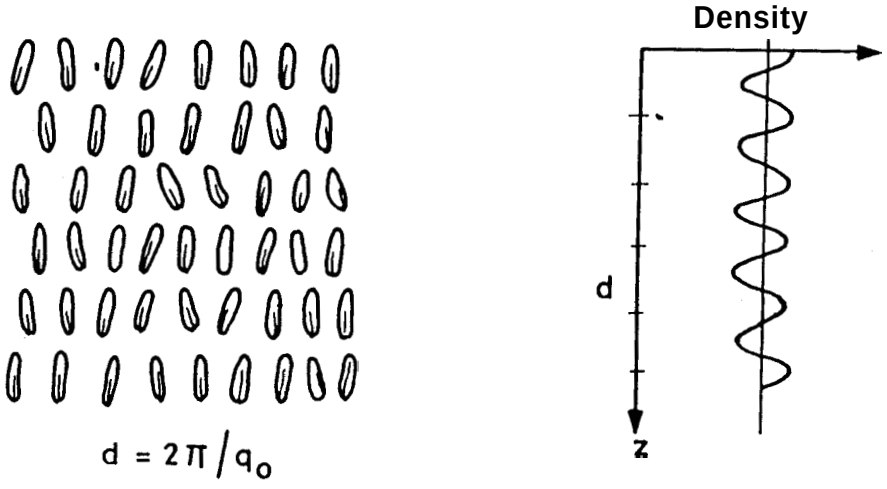

Figure 3.1

***Schematic** diagram of **the smectic A phase with its one-dimensionat' mass-density wave** along **the** average **dizection** of **the** molecular axis (Z).*

the strength of the smectic order and ρ_0 is the average density. High resolution X-ray studies on smectic A phase have revealed that the reflection corresponding to the higher order harmonics are extremely weak showing thereby that the density wave is nearly sinusoidal.[5] Accordingly, while defining an order parameter for this phase the Fourier component of the centre of mass density at only $\pm q_0 z$ is taken into consideration. Also, the lower marginal dimensionality (d_o) for the smectic A is 3 (see Ref. 6). It is known that when the spatial dimensionality, $d \leq d_o$, the fluctuations are extremely important and prevent the establishment of true long range order in one-dimension. Although this concept, referred to as the Landau-Pieirls instability,[7] has been known for some time, it has been experimentally proved for the smectic A phase only recently.[8] Thus the X-ray diffraction peak of an aligned smectic A phase is notatruly Bragg-like but has a power law decay.

For a long time only one type of smectic A phase was known wherein the layer spacing (d) is approximately equal to the length of the molecule (ℓ). However, with the synthesis of materials with a strongly polar end group, a new field of study was opened up. Madhusudana and Chandrasekhar,[9] while discussing the role played by the longitudinal dipoles in stabilizing the nematic phase proposed that the molecules with a strong dipole moment at one end of the molecule should favour an antiparallel near-neighbour arrangement. The existence of antiparallel correlations in polar

systems has been established experimentally by dielectric studies.[10] X-ray[11,12] and neutron scattering studies[13] showed that the layer spacing in the smectic A phase of alkyl as well as alkoxy cyanobiphenyls is about 1.4 times the molecular length, i.e., the structure is "bilayer" (or partially bilayer as it is more appropriately known today). This structure is schematically represented in Fig. 3.2 - the aromatic regions overlap at the centre while the alkyl chains are stretched outwards. Compounds possessing such an antiparallel arrangement of molecules exhibit interesting phenomena like reentrant behaviour[14,15] and smectic A polymorphism.[16]

Sigaud et al.[17] observed for the first time a smectic A - smectic A transition in a binary mixture of a non-polar material, viz., terephthal-bis-4-n-butylaniline (TBBA) with a strongly polar compound, viz., 4-n-pentylphenyl-4'-cyanobenzoyloxy benzoate (DB5CN). The phase diagram of this binary system is shown in Fig. 3.3. The transition between two polymorphic forms of the A phase was seen from calorimetric studies while optically no change was observed in the texture of the two A phases. Also from characteristic X-ray diffraction patterns for the two types of smectic A phases[18] the higher temperature smectic A phase has been designated as the monolayer phase (A_1) and the lower temperature A phase as the bilayer (A_2) phase.

Another type of smectic A phase referred to as the antiphase ($\tilde{A}$) was observed[19] in a binary mixture of 4'-(4-n-pentylstylyl)

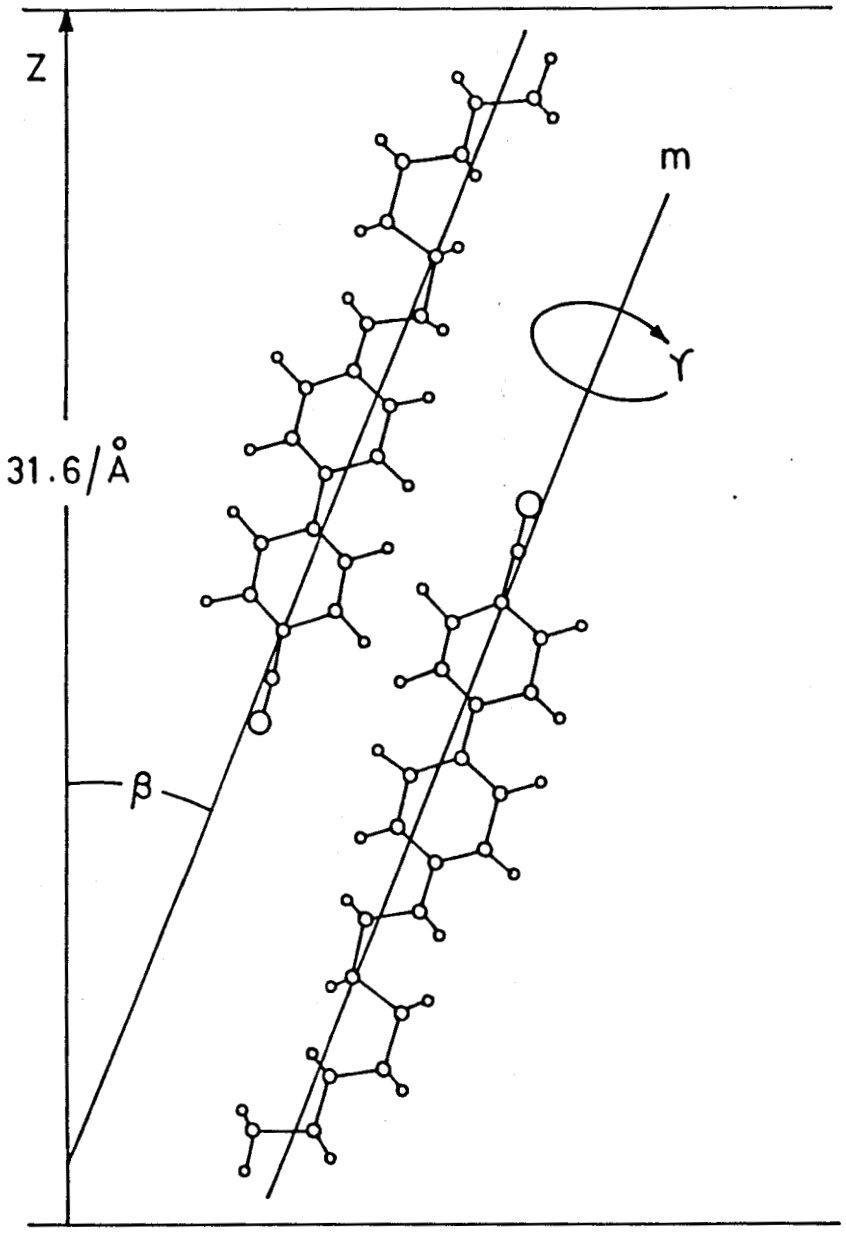

Figure 3.2

Schematic representation for **the** antiparallel arrangement **in** 8CB. (From Ref. 11).

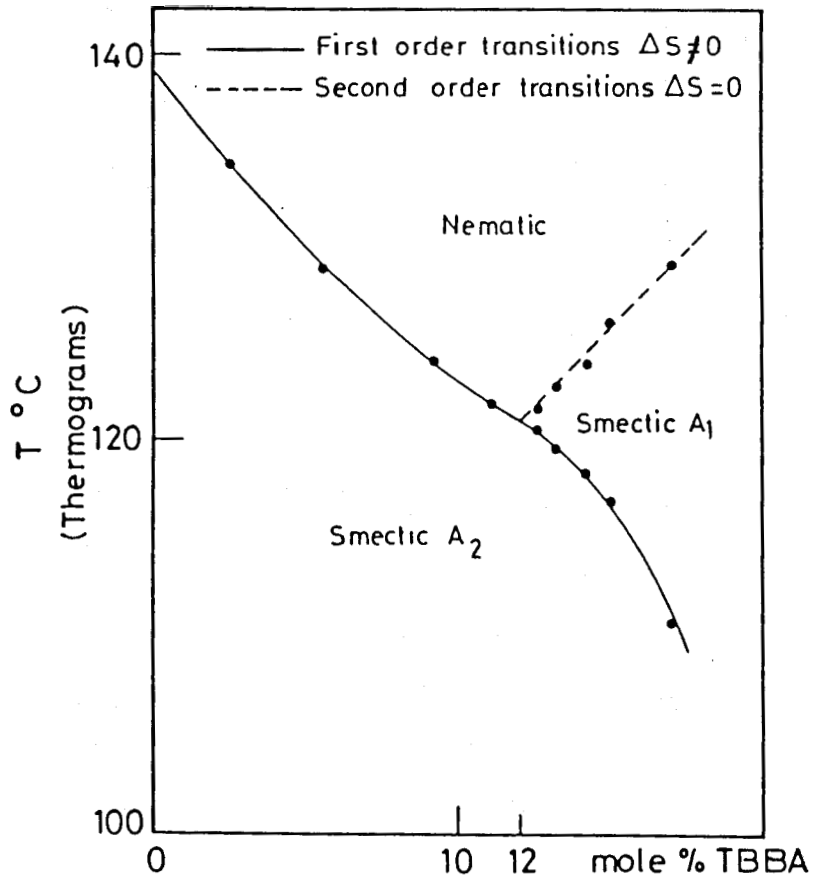

Figure 3.3

A rection of DB5CN/TBBA binary phase diagram showing the A_1-A_2 transition. (From Ref. 17).

phenyl-4"-cyanobenzoate (C5 Stilbene) and DB5CN. This was seen between the A_1 and A_2 phases. Calorimetric measurements[19] showed enthalpy changes at the A_1-$\tilde{A}$ and $\tilde{A}$-A_2 transitions while X-ray studies showed a characteristic diffraction pattern corresponding to this new phase. Optical observations made on the free surface of a droplet also showed some distinct type of defects in the $\tilde{A}$ phase both on cooling from A_1 and heating from A_2 phase. X-ray results showed that in the $\tilde{A}$ phase, the monolayer order is unperturbed, but the bilayer order oscillates periodically from one equivalent lock-in position to another resulting in a modulation of the dipolar heads within the layer. Thus $\tilde{A}$ is a biaxial phase having modulations both in the longitudinal and transverse directions.

Very recently, Levelut[20] observed another kind of smectic A phase between the $\tilde{A}$ and A_2 phases. Based on the X-ray pattern, she showed this phase to be another type of smectic antiphase possessing a non-centred rectangular lattice. It is different from the $\tilde{A}$ phase defined earlier, which has a regular rectangular lattice. This phase has been designated[2,] as the crenellated smectic A phase (A_{cre}). It has been suggested[22] that A_{cre} should always exist between the A and A_2 phases. It is relevant to mention here that quite often another type of phase, viz., the ribbon phase[23] (designated as $\tilde{C}$) intervenes between two polymorphic forms of the A phase, e.g., between A_d and A_2 or A_1 and A_2.

The schematic representation of the arrangement of the mole-

cules in these smectic A phases is given in Fig. 3.4. In the A_1 phase the layer periodicity (d) is equal to the length of the molecule (&) and accordingly it has been named as the monolayer phase. In this phase the dipolar heads are assumed to be arranged randomly within each layer. In the partially bilayer (A_d) phase, the preferential antiferroelectric ordering of the adjacent dipolar heads results in an inter-digitated layer structure whose periodicity is intermediate between ℓ and 2ℓ. The bilayer (A_2) phase has an almost perfect head-to-head arrangement of the dipolar heads, the periodicity of this phase being equal to 2Q (i.e., $d \simeq 2\ell$). In the $\tilde{A}$ phase the local order is the same as that in the A_2 phase but the direction of the dipolar arrangement alternates periodically within a layer and this results in a rectangular symmetry. The periodicity of the transverse modulations was found to be of the order of a few hundred angstroms[19] and mostly temperature independent. Just like $\tilde{A}$, the crenellated smectic A (A_{cre}) phase also shows alternation of the dipolar arrangement between two neighbouring domains but with the difference that these antiphase domains have unequal widths. It has been observed[2,] that with decrease in temperature the width of one domain increases at the expense of the neighbouring one. In the $\tilde{C}$ (or smectic ribbon phase) the layers consist of pairs of molecules showing a bilayer type of arrangement which are seen to be broken periodically by defect walls oblique with respect to the director. Thus unlike the $\tilde{A}$ or A_{cre} phases, the $\tilde{C}$ phase has an oblique lattice.

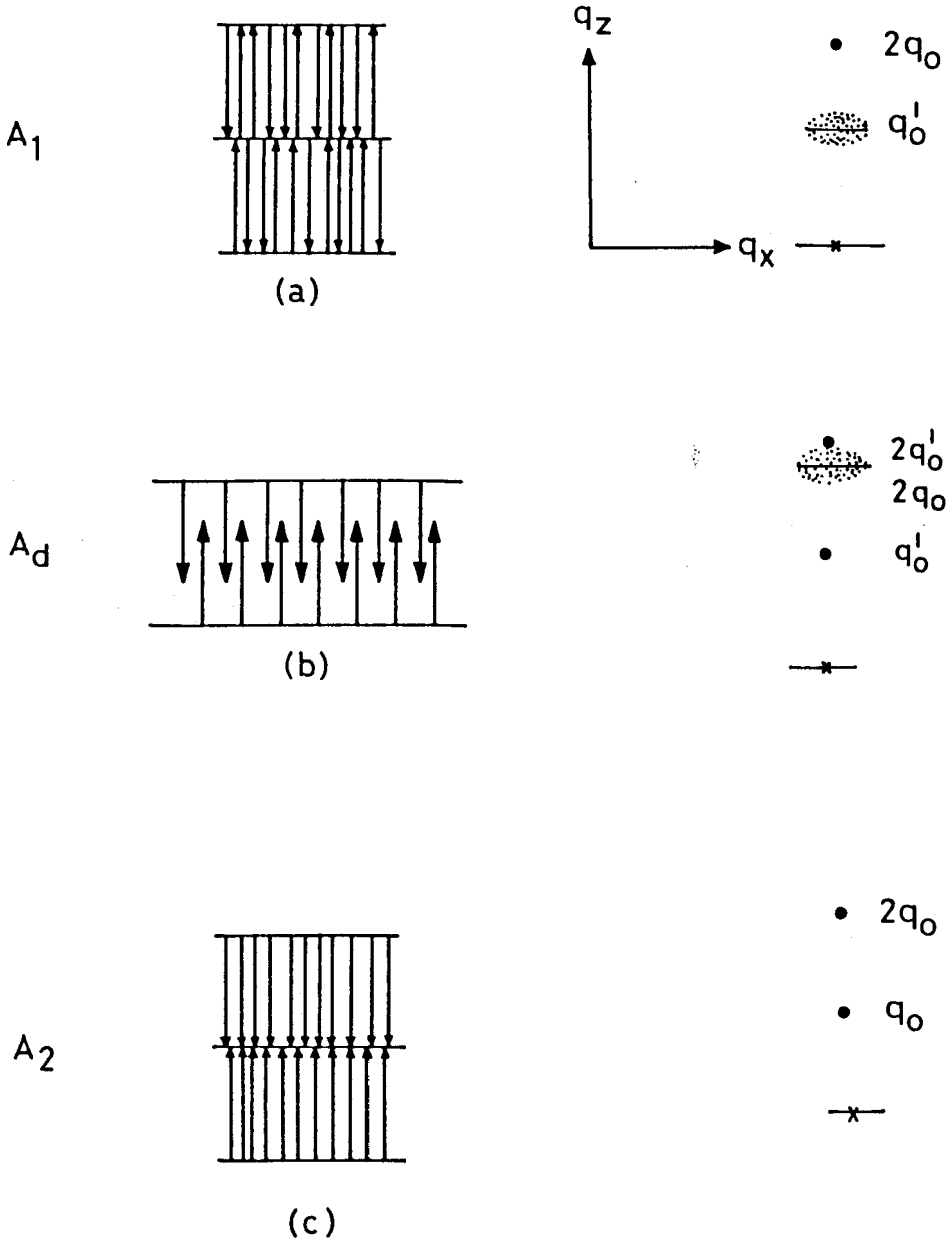

Figure_3.4a,b,c: ***Schematic representation of the molecular arrangement along with their characteristic Xray diffraction patterns for different types of smectic A phases.*** *Here (X) denotes the direct beam, (•) condensed spot, and (●) diffuse spot. (a)monolayer (A_1),(b) partially bilayer (A_d), (c) bilayer (A_2)*

.....

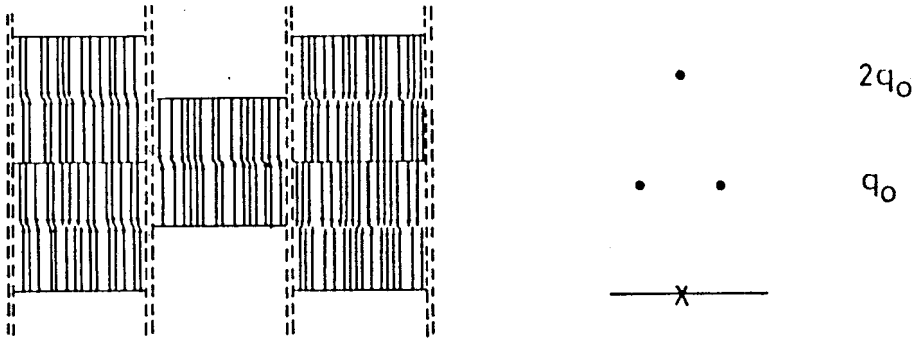

(d)

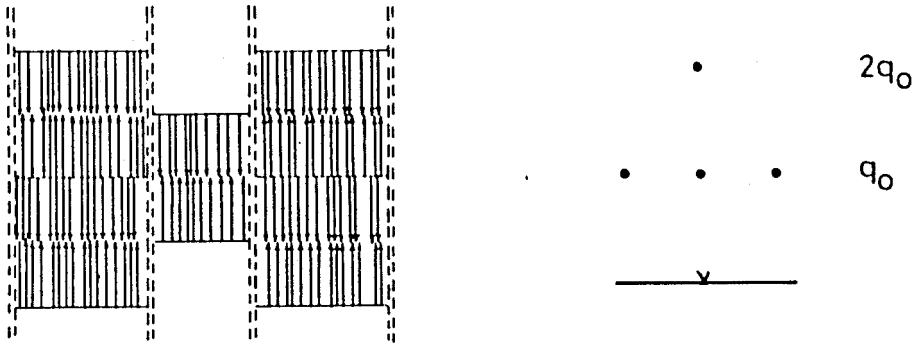

(e)

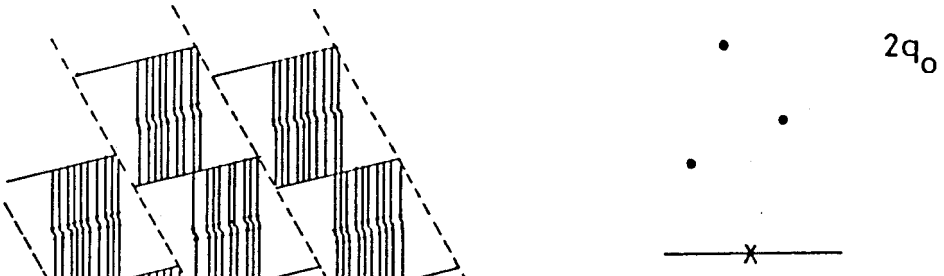

(f)

Figure 3.4d,e,f:

Schematic** representation of **the** molecular arrangement **along with** their characteristic Xray diffraction patterns for different types of smectic A phases. Here (X) denotes **the** direct **beam,
*(•) **condenbed** spot, **and** (ⓢ) diffuse **apot.** (d) smectic **antiphaae** ($\tilde{A}$), (e) crenelated smectic (A_{cre}) **and** (f) smectic **.ribbon** phase ($\tilde{C}$).*

The types of X-ray diffraction patterns to be expected from the different smectic phases are also shown schematically in Fig. 3.4.

a) The A_1 phase shows a condensed peak at $2q_0$ ($= 2\pi/\ell$) corresponding to the monolayer ordering and generally, a diffuse scattering centred around q_0' ($= 2\pi/\ell'$), which is incommensurate with respect to $2q_0$, ($\ell < \ell' < 2\ell$) (Fig. 3.4a).

b) The partially bilayer smectic A phase (A_d) shows a condensed spot at q_0', a weak second harmonic at $2q_0'$ and a diffuse peak centred around $2q_0$ (Fig. 3.4b).

c) The smectic A_2 phase shows condensed peaks at both q_0 and $2q_0$, with q_0 as the fundamental and $2q_0$ as its second harmonic (Fig. 3.4c).

d) For the $\tilde{A}$ phase there is a sharp peak at $2q_0$ and two condensed spots which are split out of the Z-axis in a direction normal to it. These off-axis spots are centred around the q_0 position (see Fig. 3.4d). In the $\tilde{A}$ phase the X-ray spots are supposed to be truly Bragg-like.[25]

e) In the A_{cre} phase a diffraction spot is observed[20] at q_0 in addition to the off-axis spots. Also, as in the $\tilde{A}$ phase, there is a condensed spot at $2q_0$ (Fig. 3.4e).

f) The X-ray patterns in the smectic $\tilde{C}$ phase show spots split

out of the Z-axis and, unlike in $\tilde{A}$, these spots are not centred around q_0. Moreover, these spots show high asymmetry in their intensities. Because the layers are tilted with respect to the Z-axis, the $2q_0$ spots are also seen off Z-axis (Fig. 3.4f).

Prost,[24] and later Prost and Barois,[25] proposed a phenomenological model to describe these different types of A phases and the transitions between them. In this model there are two fields $\rho(r)$ and $\phi(r)$ characterizing the mass density and antiferroelectric order parameters. The model incorporates two important types of terms in the free energy, viz., the elastic terms and the coupling term. The elastic terms describe the spatial modulations, corresponding to the mass density and antiferroelectric orders. These modulations are seen at collinear incommensurate wavevectors $2q_0$ and q_0' corresponding to the X-ray peaks observed in the polar nematic phase. The coupling term favours the lock-in of $2q_0$ and q_0' wavevectors and corresponds to the A_2 phase. According to the model, if the system gains energy through the coupling term, this will be at the cost of the elastic energy and vice versa. Hence the competition between these two opposing terms leads to frustration in the system. Different ways of satisfying these two terms can result in either the two-dimensional $\tilde{A}$ and $\tilde{C}$ phases or an incommensurate phase in one-dimension. Fig. 3.5 gives the wavevector representation of these phases.

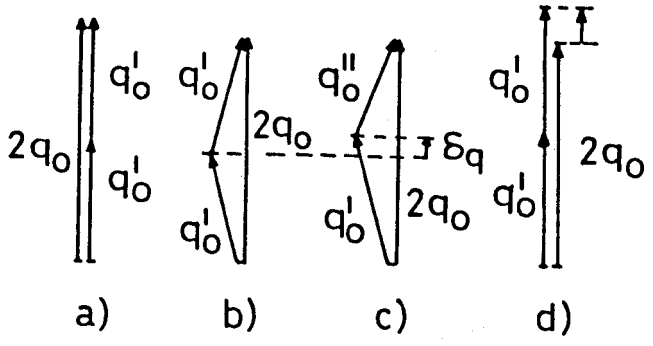

Figure 3.5

***Wavevectolr** representation of frustrated smectic phases. (a) A_2 phase, (b) $\tilde{A}$ phase, (c) $\tilde{C}$ phase, and (dl incommensulrate phase.*

Thus the model predicts a thermodynamically stable incommensurate phase. The experiments which have led to the first observation of such a phase are described in the section 3.3 of this chapter. Before presenting these results we shall discuss the phenomenological model developed by Prost and Barois[25] in somewhat greater detail in Section 3.2.

3.2 PHENOMENOLOGICAL MODEL

The smectic A phase can be characterised by expanding the Fourier series of the mass-density wave - the existence of a non-zero Fourier component at a non-zero wavevector defines the A phase. Coupling between the fundamental and the harmonic of the density modulation was first considered by Meyer and Lubensky.[26] While considering the nematic-smectic A (N-A) transition, they wrote the free energy as :

$$\Delta F = \frac{1}{2}\left[A_1 \rho_{q_0}^2 + A_2 \rho_{2q_0}^2 - D \rho_{q_0}^2 \rho_{2q_0} + \text{4th ordered terms} + \ldots\ldots\right] ,$$

where $A_1 = a_1(T - T_1)$ and $A_2 = a_2(T - T_2)$. According to them, the third order coupling between the fundamental (ρ_{q_0}) and its second harmonic (ρ_{2q_0}) in a system with saturated nematic order could drive the N-A transition to first order even though the McMillan criterion for such a system would demand a second order N-A transition. This therefore accounts for the experimental observations

on DB5CN, viz., (1) the N-A transition in this material is strongly first order even though the nematic range is large and (2) an X-ray diffraction pattern consisting of two spots one of them being the second harmonic of the other was seen. (Of course, at that time it was not realised that the A phase of this material was in fact the bilayer A_2 phase. As stated earlier, this was realised much later by Sigaud et al.[17] who observed the $A_1 - A_2$ transition.)

In order to account for the $A_1 - A_2$ transition, Prost[24] expressed the free energy by including a phase factor in the coupling term which was written as

$$D \rho_{q_0}^2 \rho_{2q_0} \cos(2\alpha - \beta)$$

The free energy can be minimised for $\alpha = \beta/2$ and $\alpha = \frac{\beta}{2} + \frac{\pi}{2}$. Defining $\gamma = 2a - \beta$, it is evident that γ can take only two values, viz., 0 and π. This binary choice for γ is equivalent to the possibilities of spin being either up or down. Thus the $A_1 - A_2$ transition is expected to belong to the n = 1, d = 3 universality class or the Ising universality class. According to this theory, whenever the fundamental (ρ_{q_0}) condenses it drives a non-zero P_{2q_0} and one obtains a bilayer smectic A phase. On the other hand, when P_{2q_0} condenses first, no bilayer order appears, i.e., $P_{q_0} = 0$. This is in agreement with the experimental observations.

Hence it is clear that the coupling between the two order

parameters is very important to describe a smectic A - smectic A transition. In a Landau picture one can replace ρ_{q_0} by any other order parameter and can still get the same basic results. If we consider molecules with a strongly polar end group, the molecules have a net electric dipole moment and as a consequence the dipolar density can be written as

$$P(r) = \frac{1}{V}\sum_i P_i \, \delta(r - r_i) \quad ,$$

where the net dipole moment of the i^{th} molecule is written as

$$P_i = \int_{V_i} r \, q(r) \, d^3 r \quad ,$$

$q(r)$ being the molecular charge density and V_i is the volume of the i^{th} molecule. Prost replaced ρ_{2q_0} by the molecular electrical potential ϕ which can be considered as an order parameter, viz., the dipolar order parameter. A state described by $\rho \neq 0$ and $\phi = 0$ does not give the same information as a state with $\phi \neq 0$. The molecular arrangement corresponding to these two cases are shown in Fig. 3.6. In the first case tails and heads are at random within a layer whereas in the second case an antiferroelectric ordering exists.

The mean field free energy can be written as

$$F = F_1 + F_2 + F_{12}$$

where F_1 and F_2 are the contributions from the two independent

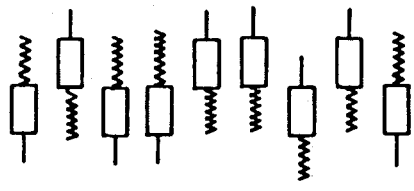

(a)

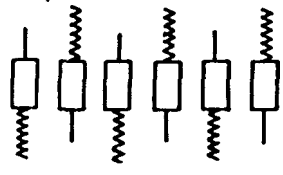

(b)

Figure 3.6

***Schematic** representation of **the** molecular **ailrangement in** smectics **with** (a) $\rho \neq 0$, $\phi = 0$, **and** (b) $\phi \neq 0$ showing **the** antiferroelectric order.* (From Ref. 25).

scalar order parameters $\rho(r)$ and $\phi(r)$ respectively and F_{12} is due to the coupling between them.

$$F_2 = \int_V \{\frac{A_2}{2}\rho^2(r) + \frac{1}{4} B_2 \rho^4(r) + \frac{C_2}{2}[(\nabla^2 + K_2^2)\rho(r)]^2\} dV \qquad (1)$$

$$F_1 = \int_V \{\frac{A_1}{2}\phi^2(r) + \frac{1}{4} B_1 \phi^4(r) + \frac{C_1}{2}[(\nabla^2 + K_1)^2 \phi(r)]^2\} dV \ , \qquad (2)$$

where $A_1 = a_1(T - T_1)$ and $A_2 = a_2(T - T_2)$. T_1 and T_2 are the mean field transition temperatures for the dipolar and mass density order parameters respectively. The conspicuous absence of the cubic terms in the free energy expressions (1) and (2) indicates that the model is for an anisotropic system. The elastic terms $\frac{1}{2} C_2 [(\nabla^2 + K_2^2) \rho(r)]^2$ and $\frac{1}{2} C_1[(\nabla^2 + K_1^2) \phi(r)]^2$ describe the presence of the density modulations $\rho(r)$ and $\phi(r)$ to be at their respective characteristic lengths $\ell' = 2\pi/K_1$ and $\ell = 2\pi/K_2$. $\rho(r)$ and $\phi(r)$ are coupled by the interaction terms in F_{12}. Up to fourth order, F_{12} can be written as

$$F_{12} = \int_V \Big\{ A_{12} \rho(r) \phi(r) + D_{12} \phi^2(r) \rho(r) + D_{21} \rho^2(r) \phi(r) + \frac{1}{2} B_{12} \rho^2(r) \phi^2(r) \Big\} dV \ . \qquad (3)$$

Even though all these terms are allowed by symmetry, not all of them are always important. The significance of the different terms depends on the mismatch between ℓ and ℓ'. If we consider $\ell' \simeq \ell$ then only $A_{12}\rho(r)\phi(r)$ and $B_{12}\rho^2(r)\phi^2(r)$ terms are relevant. If $\ell' \simeq 2\ell$, then the coupling terms $A_{12}\rho(r)\phi(r)$ and $D_{21}\rho^2(r)\phi(r)$

are not necessary and can be neglected. If the lengths mismatch totally, then the system gains energy by decoupling them.

Let us now consider the case, $\ell' \simeq 2\ell$. According to Prost and Barois[25] $\rho(r)$ and $\phi(r)$ can be defined as

$$\rho(r) = \sqrt{2}\,\rho\cos[2K_z + \beta(z)]$$

and

$$\phi(r) = \sqrt{2}\,\phi\cos[K_z + \alpha(z)] \ ,$$

where ρ and ϕ can be considered to be slowly varying functions of r. Then the free energy can be written as

$$F = \int_V \Big\{ \frac{1}{2}[A_1 + C_1(\nabla_z\alpha - \frac{q_0}{4})^2]\,\phi^2 + \frac{1}{2}[A_2 + C_2(\nabla_z\beta - \frac{q_0}{2})^2]\rho^2 + D_{12}\,\phi^2\rho\cos(2\alpha - \beta) + \frac{B_1}{4}\phi^4 + \frac{B_{12}}{2}\phi^2\rho + \frac{B_2}{4}\rho^4 \Big\} dV \qquad (4)$$

where $$q_0 = \frac{K_2 - 2K_1}{2} \ .$$

A state described by $\rho = \phi = 0$ corresponds to the disordered phase, namely, the nematic phase. In the A_1 phase, $\rho \neq 0$ and $\phi = 0$. In the A_2 phase $\rho \neq 0$ and $\phi \neq 0$ and $K_2 = 2K_1$. Thus the A_2 phase is obtained by matching ρ and ϕ wavevectors to an integer number 2. It is observed that by considering $K_2 = 2K_1$, the system gains energy through the coupling term at the cost of elastic energy. On the other hand, considering the phase matching problem in the presence of a one-dimensional order leads to the possibility of

the existence of an incommensurate phase (A_{ic}). Thus the different ways of satisfying the third order lock-in term can yield the A_2 or the A_{ic} phase.

We shall now consider only the phase dependent part of the free energy, which can be written as

$$F_{2\alpha-\beta} = \frac{1}{2}\int\left\{\frac{4C_1C_2\rho^2\phi^2)}{(C_1\phi^2 + 4C_2\rho^2)}(\nabla_z\gamma + q_0)^2 - 4D_{12}\phi^2\rho\sin^2\gamma\right\}dz \quad \ldots(5)$$

where $\gamma = \alpha - \frac{\beta}{2}$. This free energy equation is isomorphous to a classical Sine-Gordon equation and leads to the unmodulated - modulated transition as was first introduced by Frank and Van der Merwe[27] and later by de Gennes.[1,28] When the lock-in tern is larger than the elastic term, i.e., when

$$\frac{D_{12}}{q_0^2(C_1C_2)^{1/2}} > \frac{(\pi^2/4)\rho}{\phi^2(C_1/C_2)^{1/2} + 4\rho^2(C_2/C_1)^{1/2}}$$

the phase difference $\gamma = \alpha - \frac{\beta}{2}$ is constant throughout and this results in the A_2 phase. In this phase the periods of the two modulations are locked-in with a constant phase difference of 2 (see Fig. 3.7).

Let us now consider the other condition, i.e.,

$$\frac{D_{12}}{q_o^2(C_1C_2)^{1/2}} < \frac{(\pi^2/4)\rho}{\phi^2(C_1/C_2)^{1/2} + 4\rho^2(C_2/C_1)^{1/2}}$$

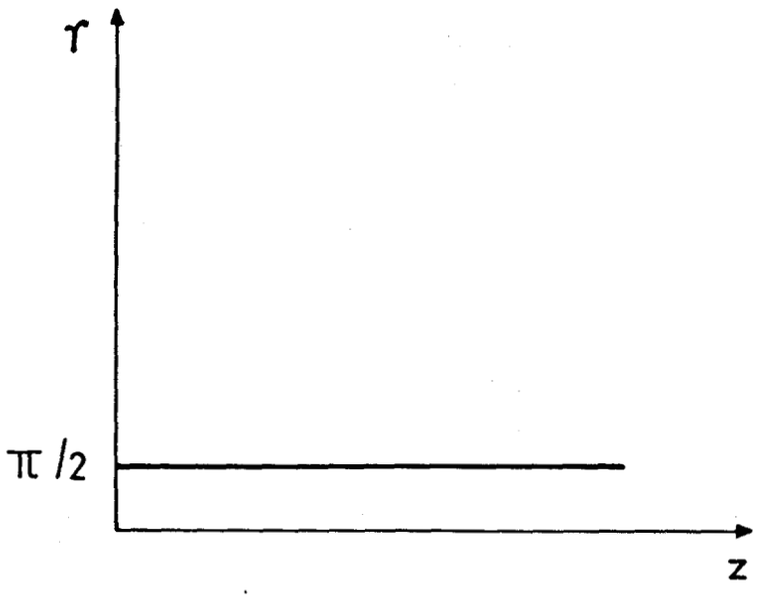

Figure 3.7

Spatial dependence of the phase difference in the A_2 phase.

Then the spatial dependence of the phase difference $(a - \frac{\beta}{2})$ is as shown in Fig. 3.8. The part over which γ is almost constant and is fixed at some specified value, corresponds to the commensurate region. It is clear from the diagram that for this region $\gamma = (2n+1)\pi/2$ for the n^{th} step. These commensurate regions are separated by discommensurate regions where the phase varies rapidly by π over a certain characteristic width. This discommensurate region which separates the successive commensurate regions are referred to as "phase solitons" and the phase which is characterized by such a structure is called as the "Incommensurate Phase".[29-31] It consists of large regions of A_2 which are periodically separated by defect walls or phase solitons in which the phase difference $a - \frac{\beta}{2}$ jumps by an amount exactly equal to π with a period Z which is the soliton periodicity. Fig. 3.9 shows the modulated structure of the soliton.

Prost and Barois have also considered the case

$$\frac{D_{12}}{q_0^2 (C_1 C_2)^{1/2}} << \frac{(\pi^2/4)\rho}{\phi^2 (C_1/C_2)^{1/2} + 4\rho^2 (C_2/C_1)^{1/2}}$$

the phase difference γ tends to show a linear variation as shown in Fig. 3.10. This refers to the weak coupling limit, i.e., the coupling energy becomes very weak compared to the elastic energy. Now ρ and ϕ orders can develop independently and are supposed to be coupled only through the fourth order terms. A schematic representation of the weakly coupled or percolated type of incommensurate A phase has been given by Prost and Barois. This is reproduced

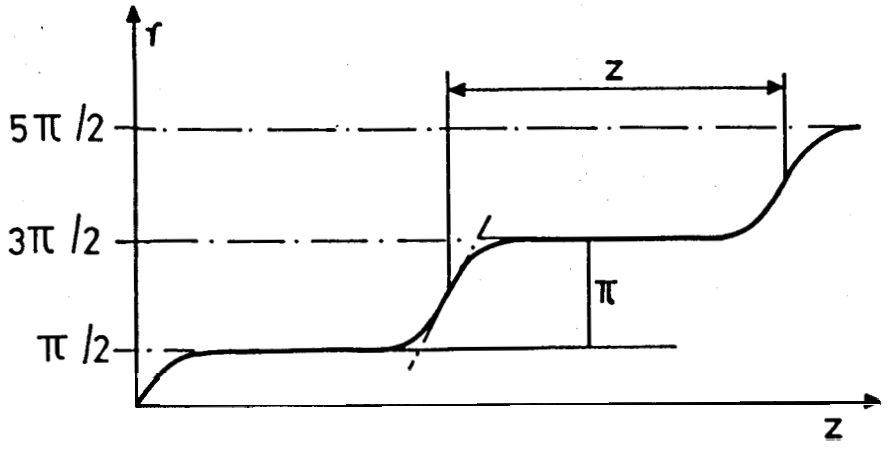

Figure 3.8

Spatial dependence of the phase teim for the strongly coupled incommensurate phase.

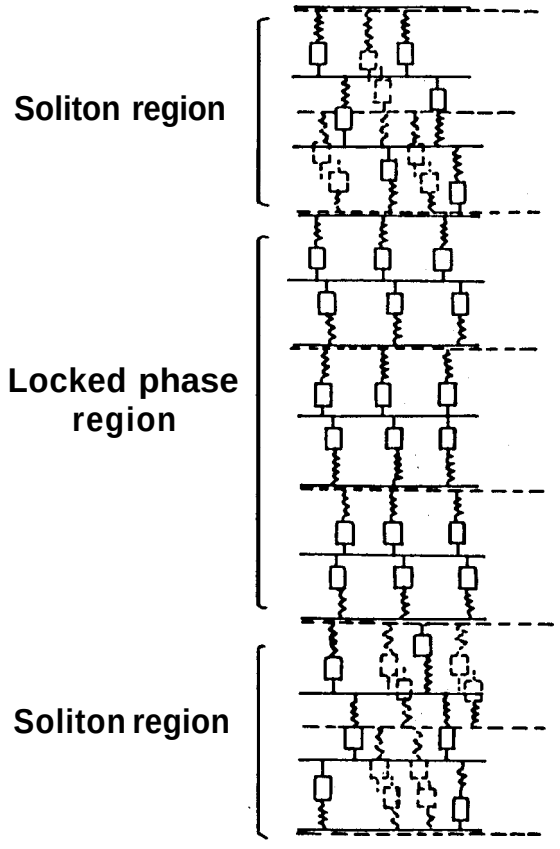

Figure 3.9

***Schematic** representation of **the** arrangement of **the** molecules **in the** strongly **coupled** incommensurate **phase.** (From Ref. 25).*

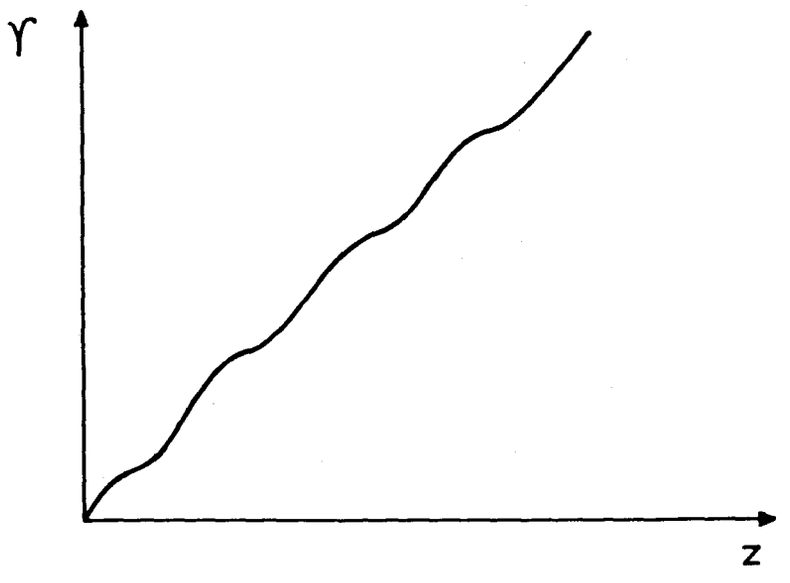

Figure 3.10

Spatial dependence of the phase difference in the weakly coupled incommensurate phase. (From Ref.30).

in Fig. 3.11. Thus Prost and Barois have, on the basis of their phenomenological theory, predicted the existence of an incommensurate smectic A phase, i.e., a smectic A phase with two incommensurate collinear periodicities. However such a phase was not seen experimentally. The only case reported to date of a smectic with two coexisting incommensurate density modulations is the three dimensionally ordered smectic E phase of 4-octyl-4'-cyanoterphenyl.[32]

In this chapter, we present the results of our X-ray studies on a binary system. These results which have led to the first observation of a fluid incommensurate phase (designated as A_{ic}) will be presented in the next section.

3.3 EXPERIMENTAL

Materials

The materials studied were 4-n-heptyloxyphenyl-4'-cyanobenzoyloxy benzoate (DB7OCN) and its mixtures with 4-n-octyloxy-4'-cyanobiphenyl (8OCB). The molecular structures as well as the transition temperatures of the two compounds are given in Fig. 3.12.

X-ray Set Up

X-ray studies have been conducted using the set up described in Chapter II. Monochromatic copper K_α-radiation and a flat photographic film which is located at the focus of the monochromator (bent quartz crystal) served as the source and the detector respec-

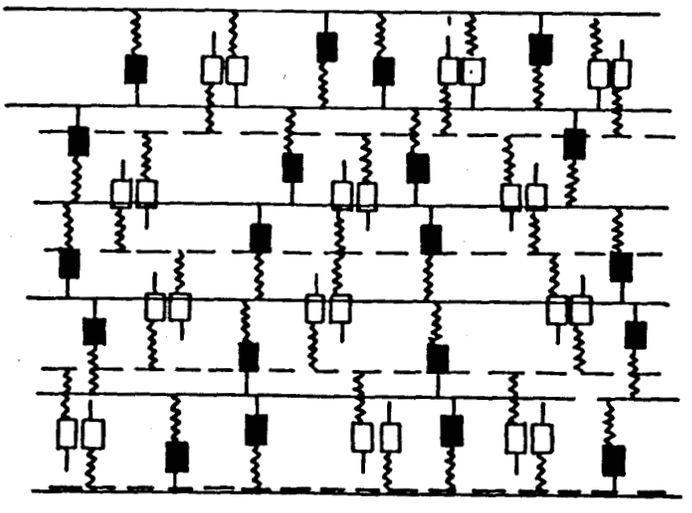

Figure 3.11

Schematic representation of weakly coupled incommensurate phase showing the exintence of two interpenetrating incommensurate peziodicitien correhponding to the molecular length (solid molecules) and pair length (open molecules). (From Red. 25).

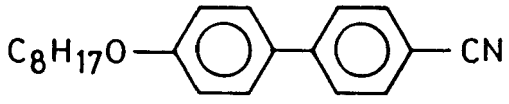

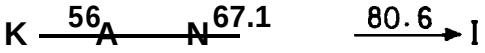

4-octyl-4'-cyanobiphenyl (8OCB)

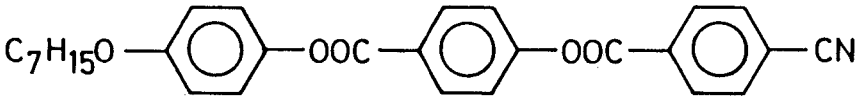

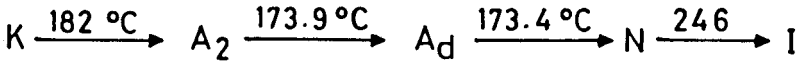

4-n-heptyloxyphenyl-4'-cyanobenzoyloxybenzoate (DB7OCN)

Figure 3.12

The chemical structures of 8OCB and DB7OCN along with the transition temperatures.

tively. Tne sample was taken in a Lindemann glass capillary (0.5 mm dia) whose ends were sealed after filling the sample. The substance was always heated to the nematic phase and then cooled in the presence of a aagnetic field (0.5 T) into the smectic A_d phase to get an oriented sample. To get a perfect monodomain sample in the incommensurate phase (A_{ic}) it was necesary to cool the sample at a very slow rate (1°C/hr) through the A_d phase till the A_{ic} phase was formed. A typical exposure at any temperature took about 20 minutes during which the temperature was maintained to ±100 mK. The accuracy in the determination of layer spacing was ± 0.1 Å or better.

3.4 RESULTS AND DISCUSSION

The partial temperature-concentration (T-X) diagram of the DB70CN-80CB binary system is shown in Fig. 3.13. It is seen that for mixtures with 80CB concentrations (X) up to 24%, there is the $A_d - A_2$ transition. For X > 24%, the incommensurate A (A_{ic}) phase intervenes between the A_d and A_2 phases. This phase diagram has been obtained using a combination of optical microscopy, DSC and X-ray methods. The $A_d - A_2$ transition was not detectable optically but could be seen both by DSC and X-ray experiments. On the other hand, the $A_d - A_{ic}$ and $A_{ic} - A_2$ transitions were not detected by DSC but could be obtained by optical microscopy as well as X-ray studies. Optical studies showed that on cooling the sample from the A_d phase zig-zag folds appear on the back of the focal conic

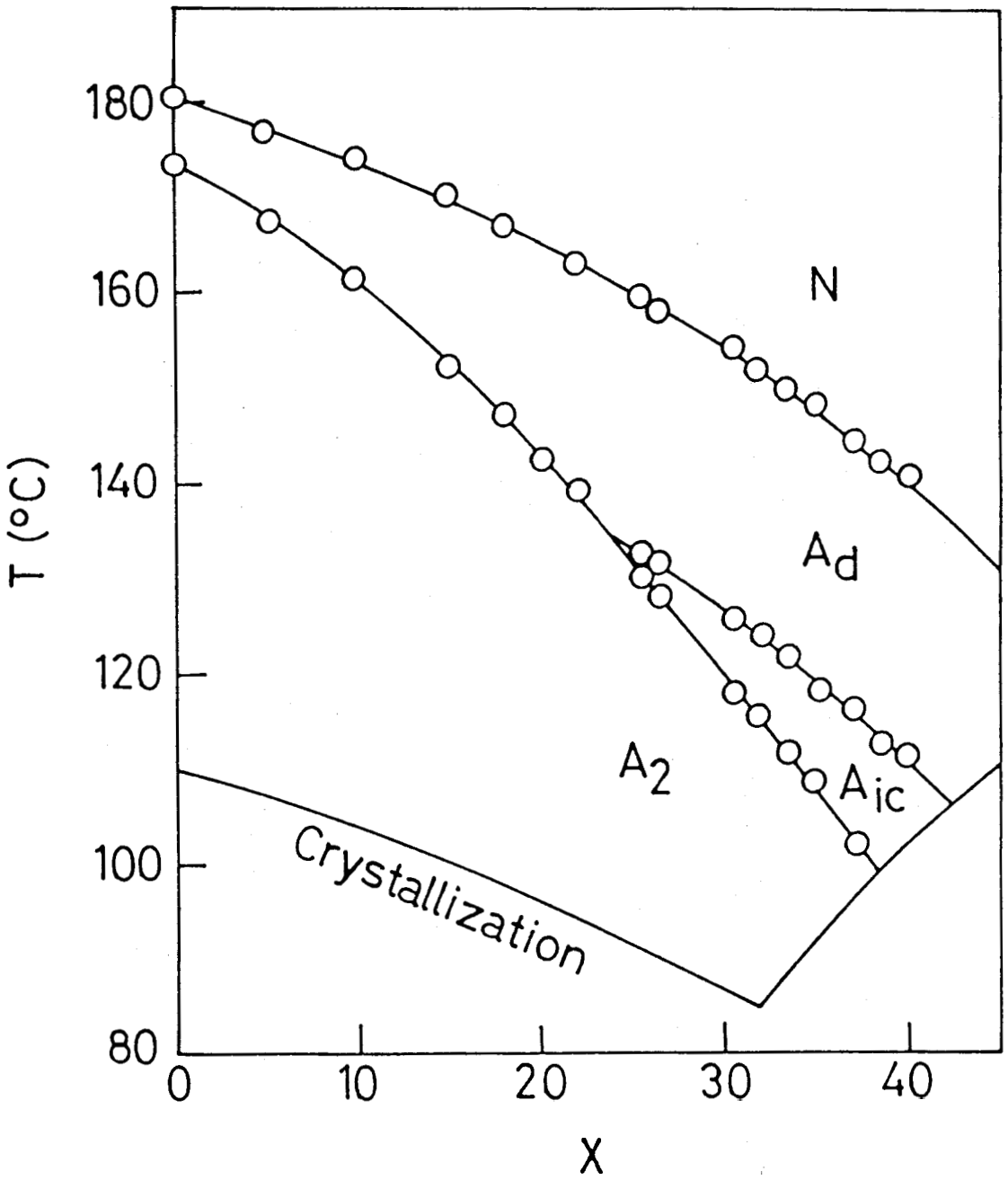

Figure 3.13

Partial temperature-concentration diagzam for vazying mol % (X) of 8OCB in DB7OCN.

fans at the $A_d - A_{ic}$ transition (see Fig. 3.14). These become prominent well in the A_{ic} phase and disappear at the $A_{ic} - A_2$ transition. On the other hand, on cooling a homeotropically aligned A_d phase, the A_{ic} phase makes a dramatic appearance in the form of loops as shown in Fig. 3.15. These defects do not completely clear off in the A_2 phase. When the sample is heated back into the A_{ic} phase, a burst of parabolic focal conic like defects[33] appear at the $A_2 - A_{ic}$ transition which do not clear off completely in the A_d phase. We shall now discuss the results of the X-ray investigations.

X-ray Studies

We have carried out layer spacing measurements for several concentrations as a function of temperature. For all those concentrations which do not exhibit the A_{ic} phase, the $A_d - A_2$ transition is seen as a change in the slope of the layer spacing (d) versus temperature plot. Fig. 3.16 shows the thermal variation of the layer spacing near the $A_d - A_2$ transition for the X = 18% mixture. In the A_d phase, the layer spacing shows an increase with decrease in temperature, the rate of variation increasing as the A_2 phase is approached. In the A_2 phase the layer spacing shows a small linear increase with decrease in temperature. It may be recalled that Hardouin et al.[34] observed the $A_d - A_2$ transformation in DBnOCl homologous series only through a similar thermal variation of layer spacing, the slope change signifying the transition.

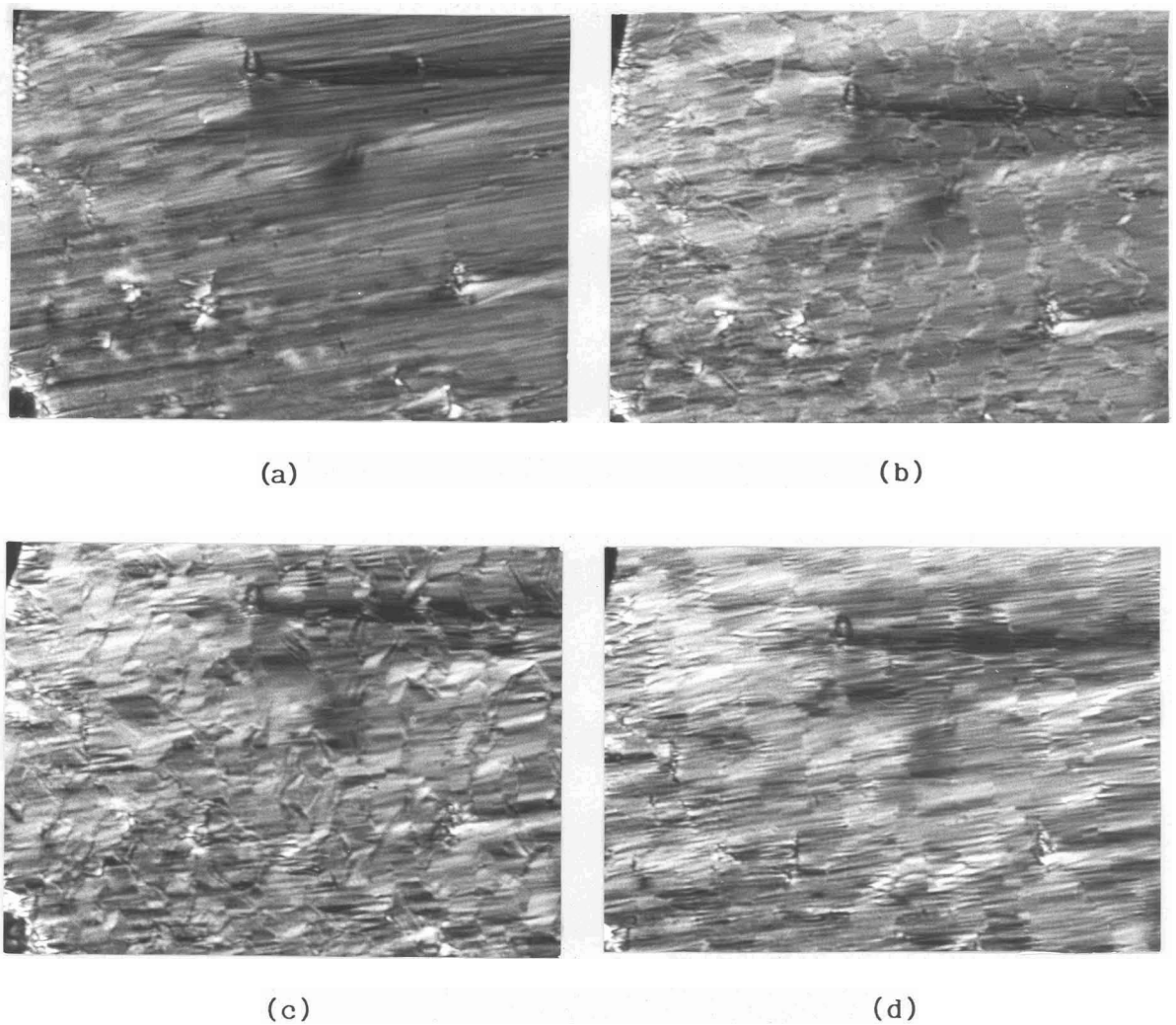

Figure 3.14

Optical textures obtained on cooling a focal conic region of the A_d phase: (a) A_d phase T = 120°C, (b) at the A_d-A_{ic} transition T = 115.5°C, (c) A_{ic} phase T = 113.5°C, and (d) A_2 phase T = 105°C.

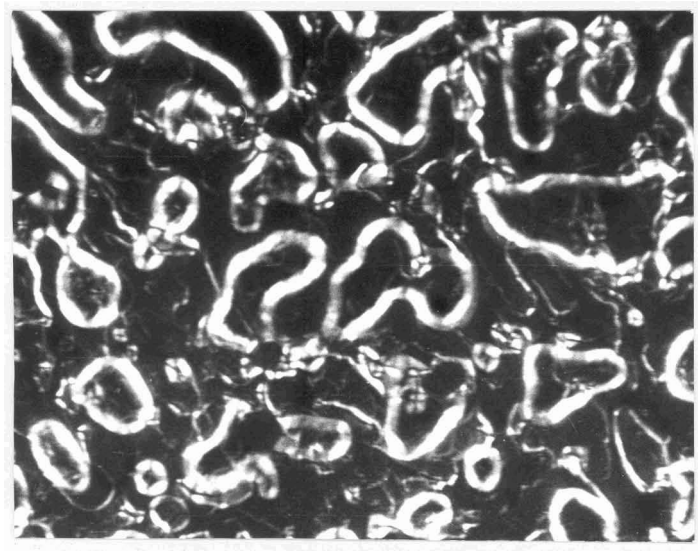

(a)

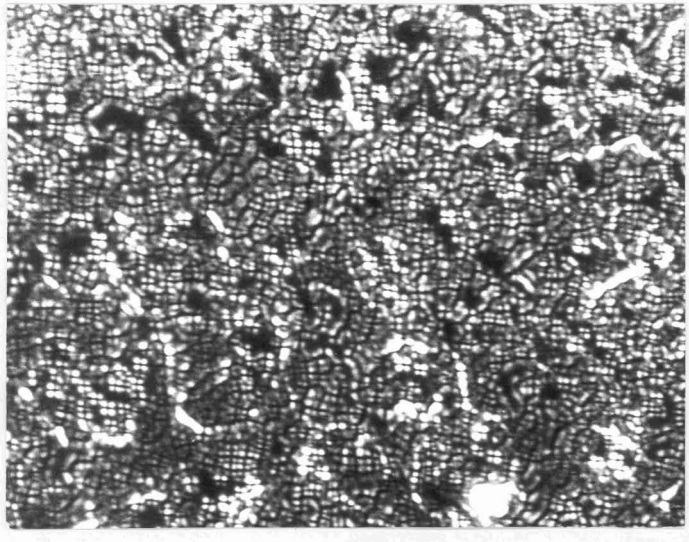

(b)

Figure 3.15

Optical textures in the A_{ic} phase obtained on (a) cooping from a homeotropically aligned A_d phase T = 113°C, and (b) heating from the A_2 phase T = 108.5°C.

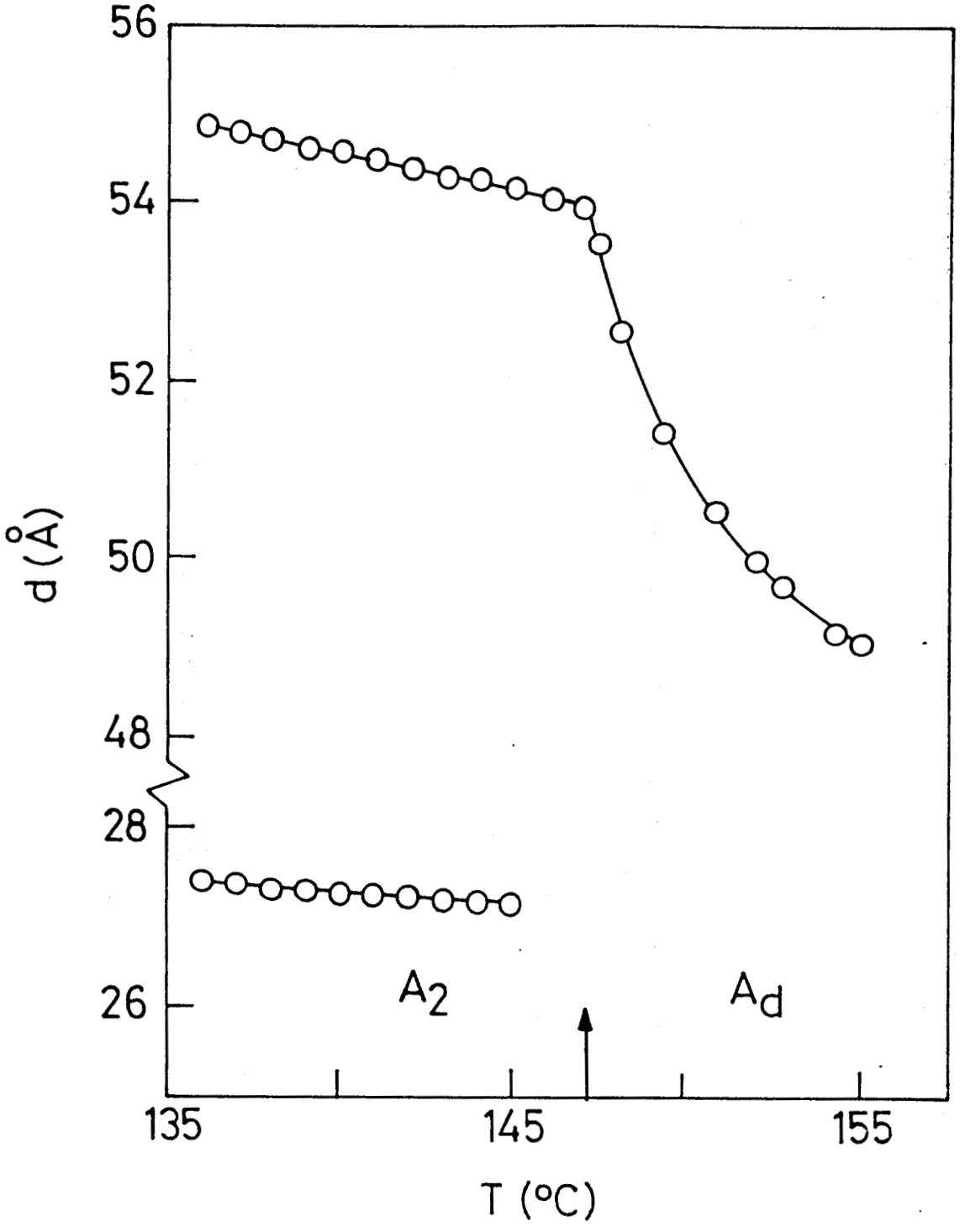

Figure 3.16

Temperature variation of the lager spacing (dl *in the* A_d *and* A_2 *phases for X = 18 mol %.*

The thermal evolution of the layer spacing corresponding to the A_d, A_{ic} and A_2 phases for the 34.8% mixture is shown in Fig. 3.17. In the A_d phase the layer spacing ($d = 2\pi/q_0'$) increases with decrease of temperature. The on-set of the incomensurate (A_{ic}) phase is signalled by the appearance of reflections corresponding to q_0 and $2q_0$. Thus the characteristic diffraction pattern of the A_{ic} phase has 3 spots, corresponding to wavevectors q_0, q_0' and $2q_0$. The variation of $2\pi/q_0'$ in the A_{ic} phase is opposite to that in the A_d phase - d decreases with decreasing temperature throughout the A_{ic} phase while it increases in the A_d phase. $2\pi/q_0$ and its second harmonic $2\pi/2q_0$ also show a decrease, albiet less pronounced than that of $2\pi/q_0'$, in the A_{ic} phase. At the A_{ic} - A_2 transition, $2\pi/q_0'$ disappears and both $2\pi/q_0$ and $2\pi/2q_0$ reverse their trend, i.e., they start increasing with decreasing temperature.

It should be mentioned that we did not see any reflections corresponding to combinations of q_0 and q_0' even after very long exposures. (The set up did not allow very low angle reflections ($< 0.5°$) to be recorded.) Also it was verified that the high angle diffraction ring was diffuse in all the three phases, viz., A_d, A_{ic} and A_2 phases showing thereby that the in-plane order is liquid-like in these phases.

Microdensitometer scans taken along the Z-axis of a series of representative photographs for the X = 35% mixture are given in Fig. 3.18. Fig. 3.18a shows a sharp peak at q_0' corresponding

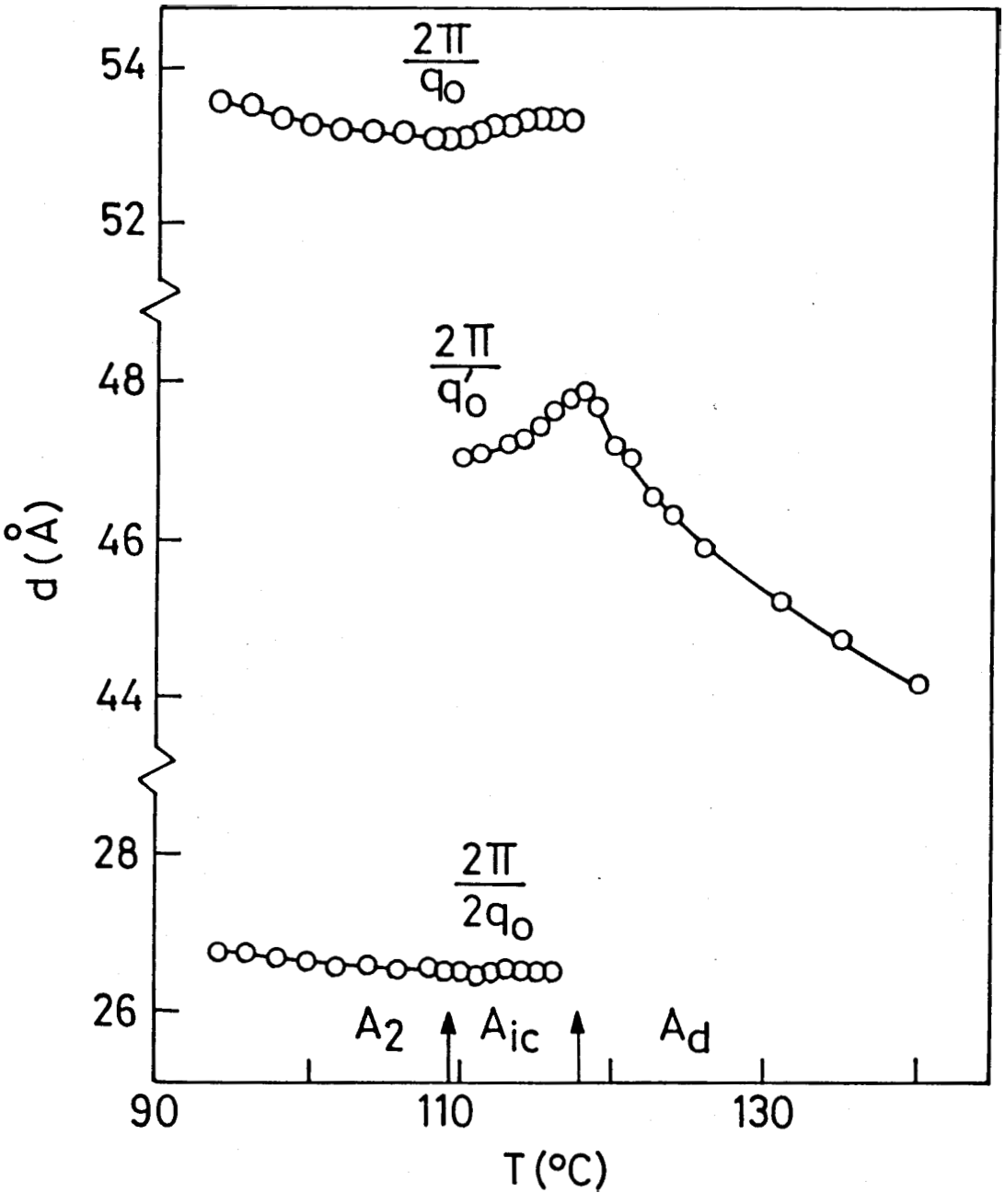

Figure 3.7 7

Thermal variation of the lager opacing (d) in the A_d, A_{ic} and A_2 phases for X = 34.8% mixture.

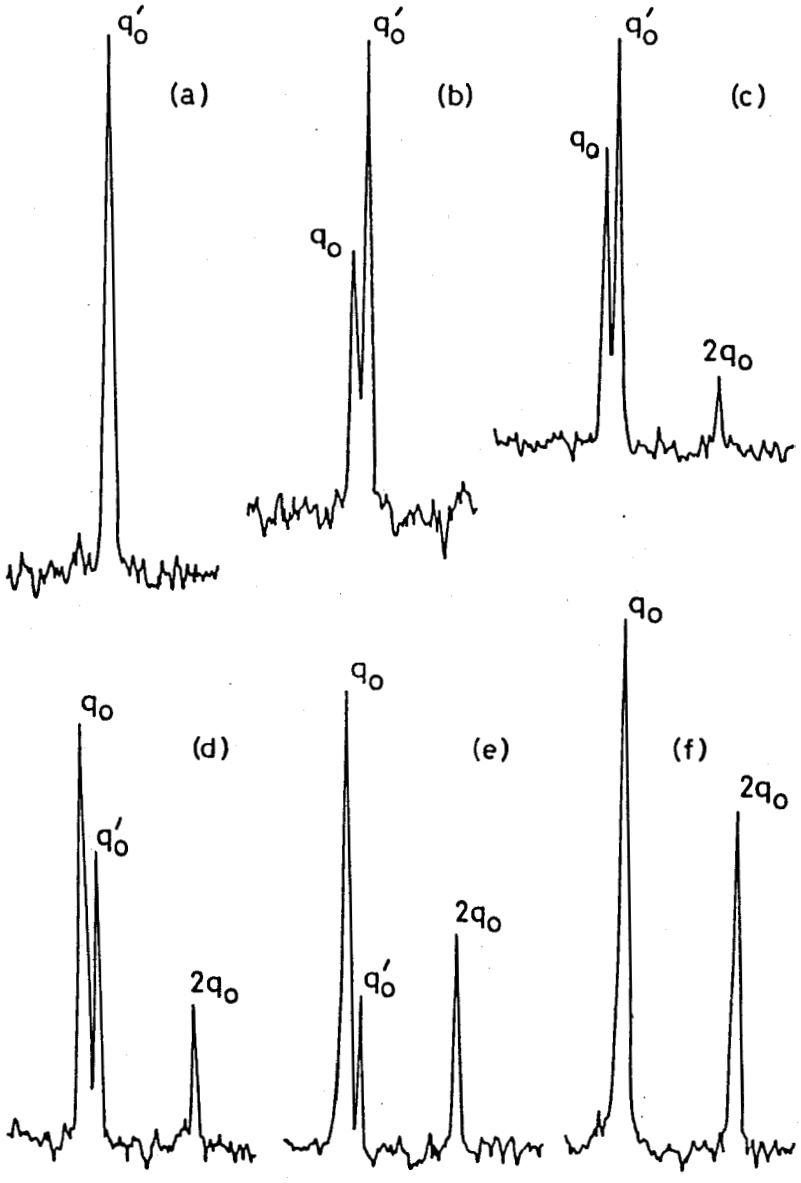

Figure 3.18

Microdensitometer scans of the X-ray diffraction photographs taken along the Z-axis for X = 34.8 mol % mixtuze at (a) 119°C in the A_d phase, (b)-(e) 117, 116, 114.50, and 112°C in the A_{ic} phase and (f) 106°C in the A_2 phase.

to the A_d phase at 119°C. On cooling, a second sharp peak is seen at q_0 close to q_0' (Fig. 3.18b). This corresponds to the onset of the A_{ic} phase. On further cooling the intensity of the reflection at q_0' decreases while that at q_0 increases with an accompanying increase in the intensity of the second harmonic at $2q_0$. Figs. 3.18c and d show the switch over of the relative strengths of q_0' and q_0 reflections. Finally at 108°C the peak at q_0' disappears leaving a clear signature of the A_2 phase - strong reflections at q_0 and $2q_0$ (see Fig. 3.18f). It should be emphasized here that regardless of their amplitudes, the sharpness of these reflections remains the same at all temperatures.

The question may be asked whether the different modulations observed in the A_{ic} phase are truly collinear. In order to ensure that this is the case, X-Y intensity contour diagrams of several pictures taken in the A_{ic} phase were mapped using a X-Y microdensitometer (Joyce-Loebl Scandig 3 in conjunction with an on-line computer). A typical contour diagram is reproduced in Fig. 3.19. The widths of the diffraction spots are 0.8 x 10^{-2} $\mathring{A}^{-1}$ in the z-direction and 1.7 x 10^{-2} $\mathring{A}^{-1}$ in the X-direction. The slightly higher width in the X-direction arises from the geometry of the X-ray monochromator set up. However, it is evident that any displacements of the reflections along the X-axis arising from a lateral periodicity of several hundred angstorms would have been revealed from the contours. It is therefore clear that the three diffraction

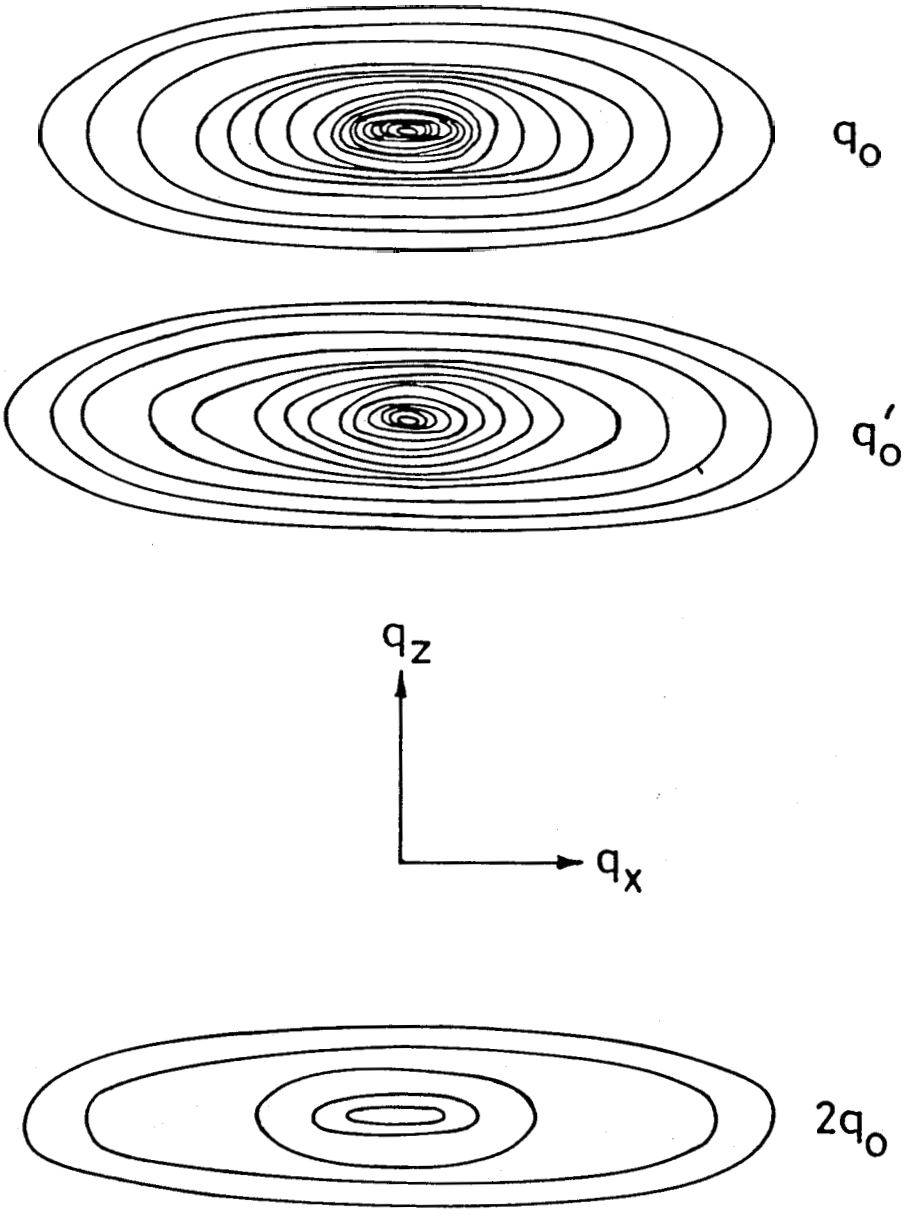

Figure 3.19

Intensity contour map of a Xray diffraction photograph taken for the X = 34.6 mol % mixture at 115.5°C. Widths of the spots are discussed in the text. The spot at $2q_0$ has been displaced closer to the other two spots for convenience.

spots are indeed collinear along the z-axis. Thus we have observed the incommensurate smectic A phase.

The variation of the layer spacing (d) in the A_d and A_{ic} phases were measured for 5 different concentrations, (X = 26.5, 32.0, 35.0, 37.5 and 41.0%) all of which show the A_{ic} phase. These data which are shown in Fig. 3.20 have been collected by taking sufficient care to see that the absolute accuracy of the layer spacing for any concentration is reproducible to within ± 0.1 Å. (We shall see later that this reproducible accuracy in the absolute determination of d for any concentration is very important). It is seen from Fig. 3.20 that essentially the same behaviour is seen for all the concentrations.

It can be argued that the A_{ic} phase might perhaps be a two-phase region consisting of regions of A_d and A_2 and hence the diffraction in the two phase region should be nothing but the superposition of the diffraction patterns of the two individual phases. We shall assume A_{ic} to be a two-phase region and then discuss the layer spacing variation that is expected in that case. Consider the schematic diagram of Fig. 3.21. In such a case let us consider a tie line MN (as shown in Fig. 3.21 - a constant temperature line parallel to the concentration axis and connecting the $A_d - A_{ic}$ and $A_{ic} - A_2$ boundaries (marked 1 and 2 in the figure). It is well known[35] that for all concentrations along such a tie line the layer spacing corresponding to the A_d and A_2 modulations are given

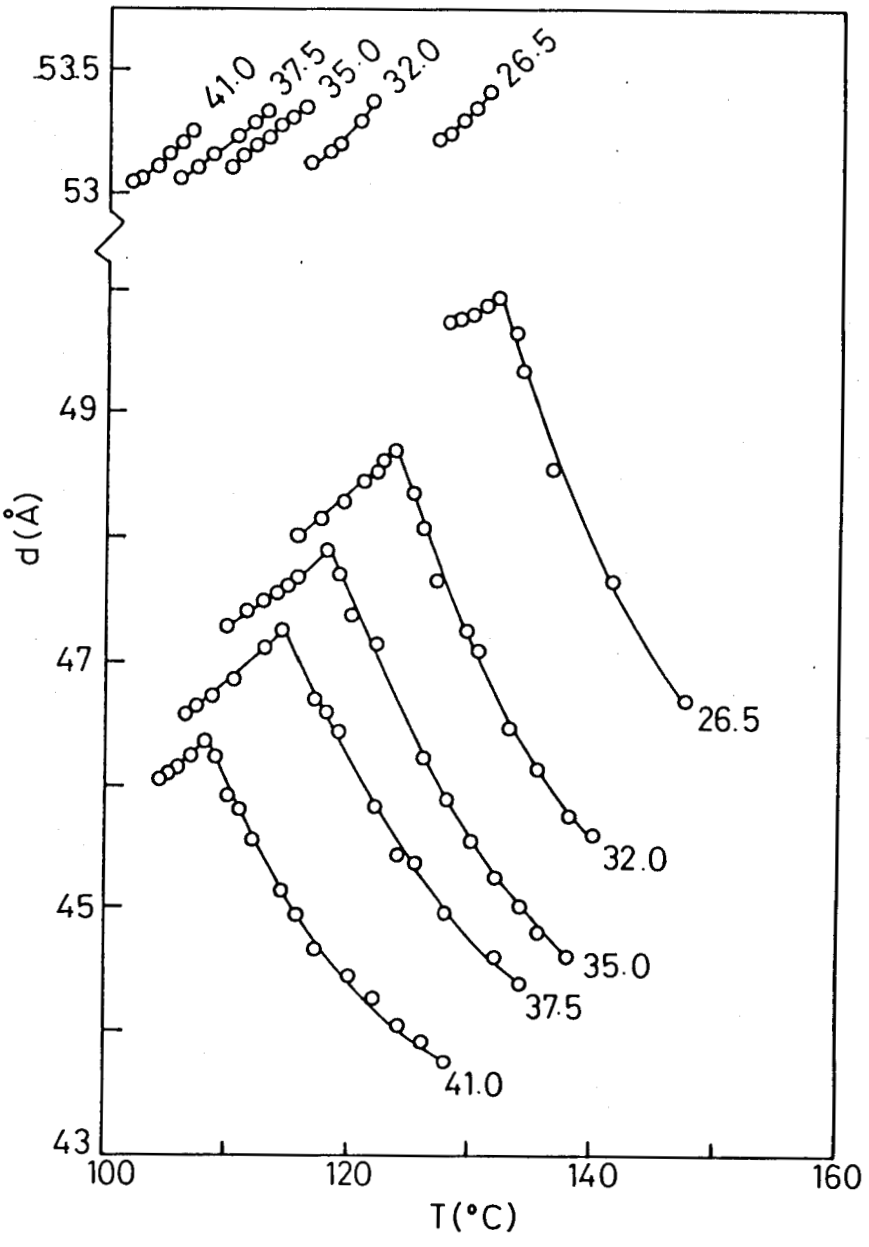

Figure 3.20

Experimental variation of the layer rpacing with the temperature for different concentzationr of 8OCB in the A_d *and* A_{ic} *pharer.*

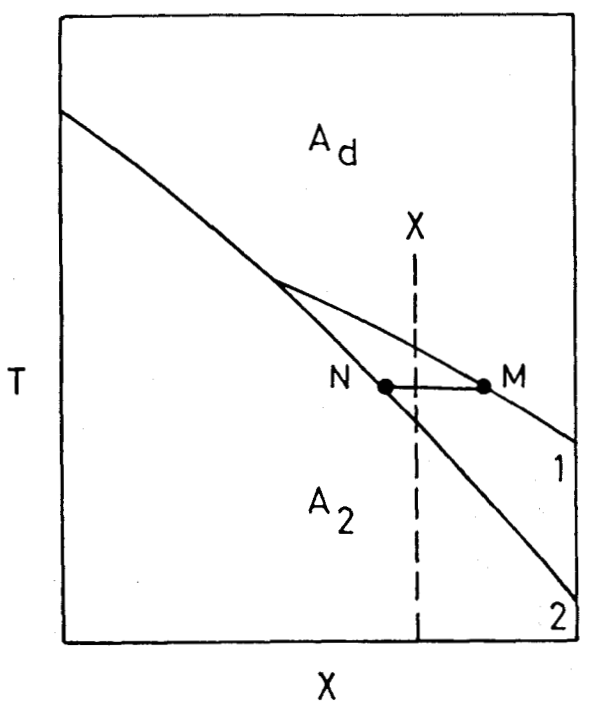

Figure 3.21

***Schematic T-X** diagram of phase boundaries in the .region of existence of A_{ic}. In the event of A_{ic} being a two-phase zegion, NM corresponds to a 'tie-line' which intersects the A_d-A_{ic} and A_{ic}-A_2 boundaries marked 1 and 2 at M and N respectively.*

by the values at M and N respectively. In other words for any concentration the temperature variation of the layer spacing in the two phase region are uniquely determined[36] by the variations along the boundaries 1 and 2. This also implies that the layer spacing evaluated at any common temperature should be independent of the concentration. This is schematically represented in Fig. 3.22. It is clear that for every concentration the data for $2\pi/q_0'$ in the two phase region should fall on the same curve. This argument holds good for $2\pi/q_0$ also. On the contrary, the experimental data shown in Fig. 3.20 for five concentrations (X = 41%, 37.5%, 35%, 32% and 26.5%) in the A_d and A_{ic} phases show that at any temperature in the A_{ic} phase there is a clear change in the layer spacing with concentration which is contrary to what is expected if A_{ic} was a two-phase region. In fact, we find that the layer spacing corresponding to the q_0 modulation at any temperature in the A_{ic} phase is higher for a higher concentration of the shorter molecular species, viz., 8OCB. Thus the possibility of the A_{ic} phase being a two phase region is definitely ruled out.

DSC Studies

Fig. 3.23 shows the differential scanning calorimetry runs for pure DB7OCN while those for DB7OCN and 80CB mixtures are shown in Fig. 3.24. These runs have been presented after normalizing to unit weight of the sample so that they can all be directly compared. All these exotherms were recorded at 0.5°C/min cooling rate and 0.5 mcal/sec sensitivity. The sample was allowed to equilibriate

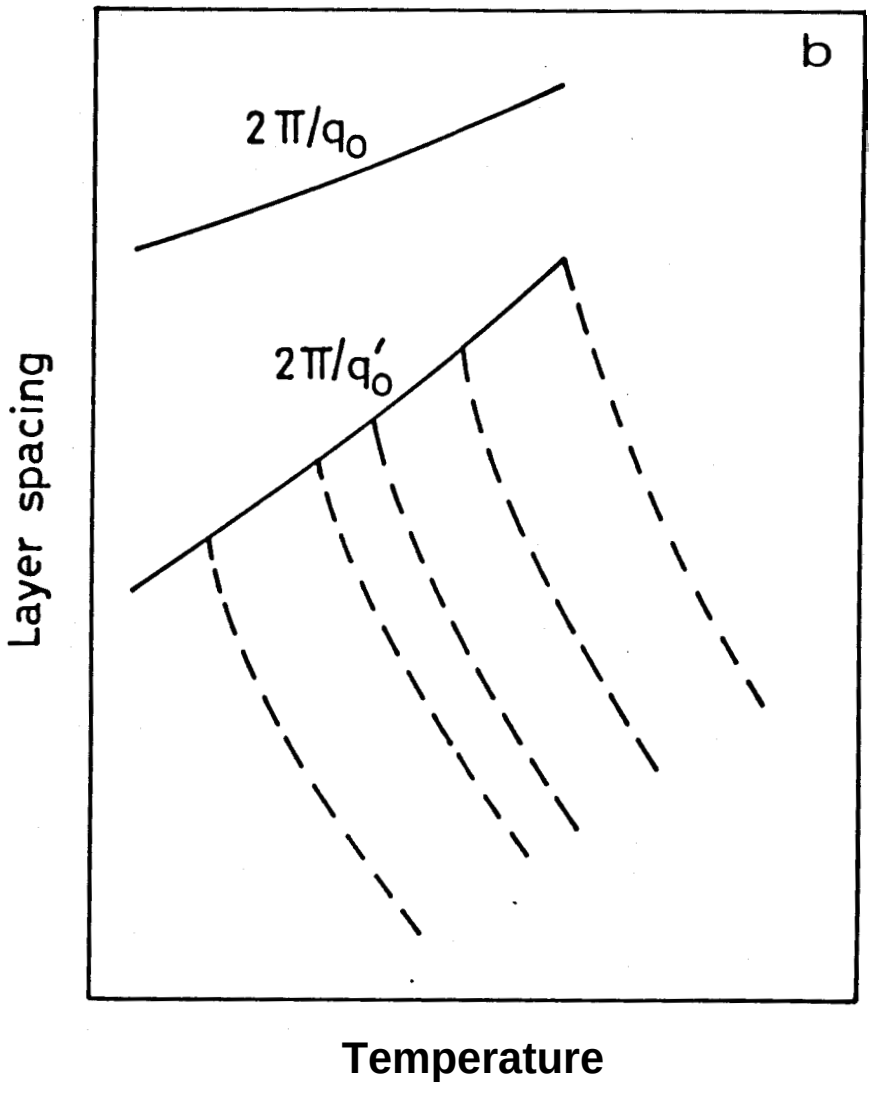

Figure 3.22

Schematic representation of the expected temperature variation of the layer opacingo (solid curves) for different concentrationo if the A_{ic} phase weze a two phase zegion consisting of A_2 and A_d regions. The dashed curves show the experimental vaziation in the A_d phase.

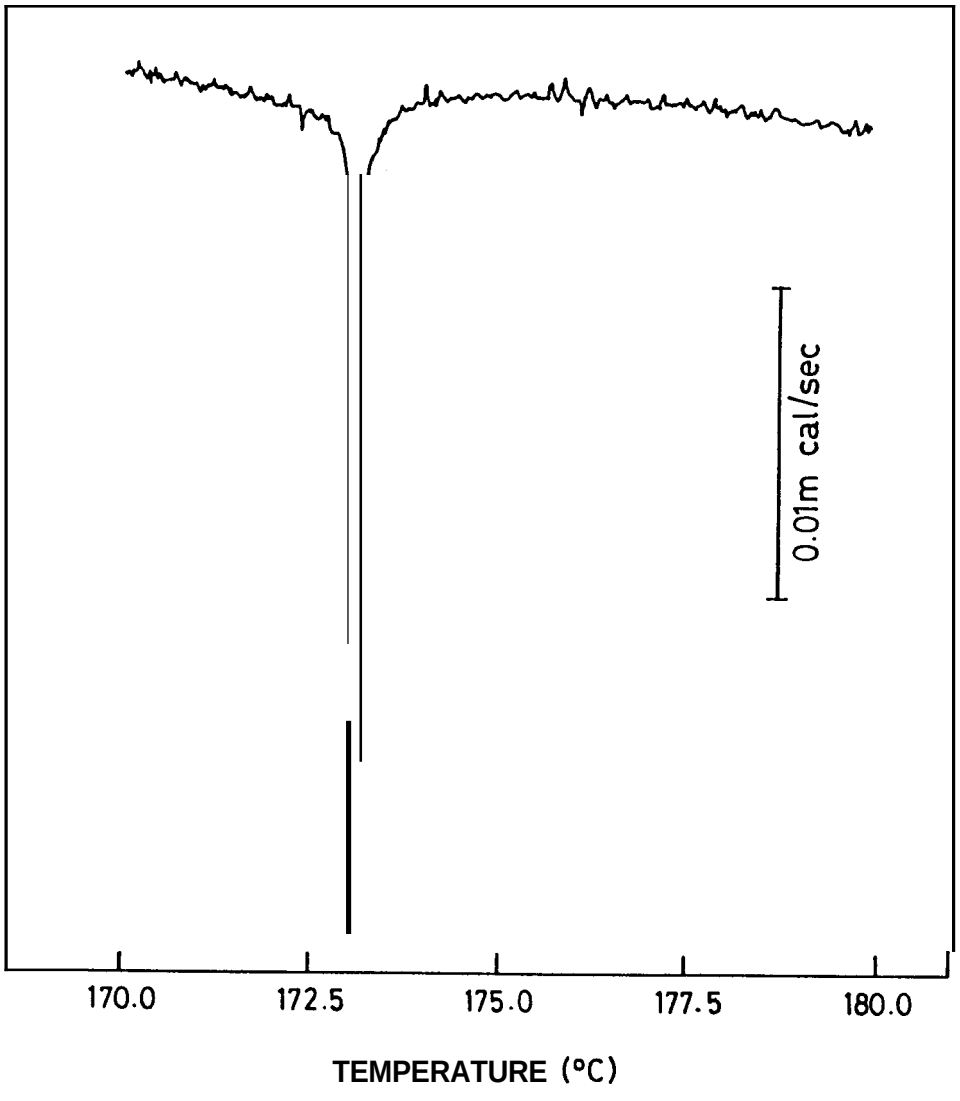

Figure 3.23

DSC scan for pure DB7OCN nhowing the A_d-A_2 transition, taken in the cooling mode at 0.5°C/min. rate.

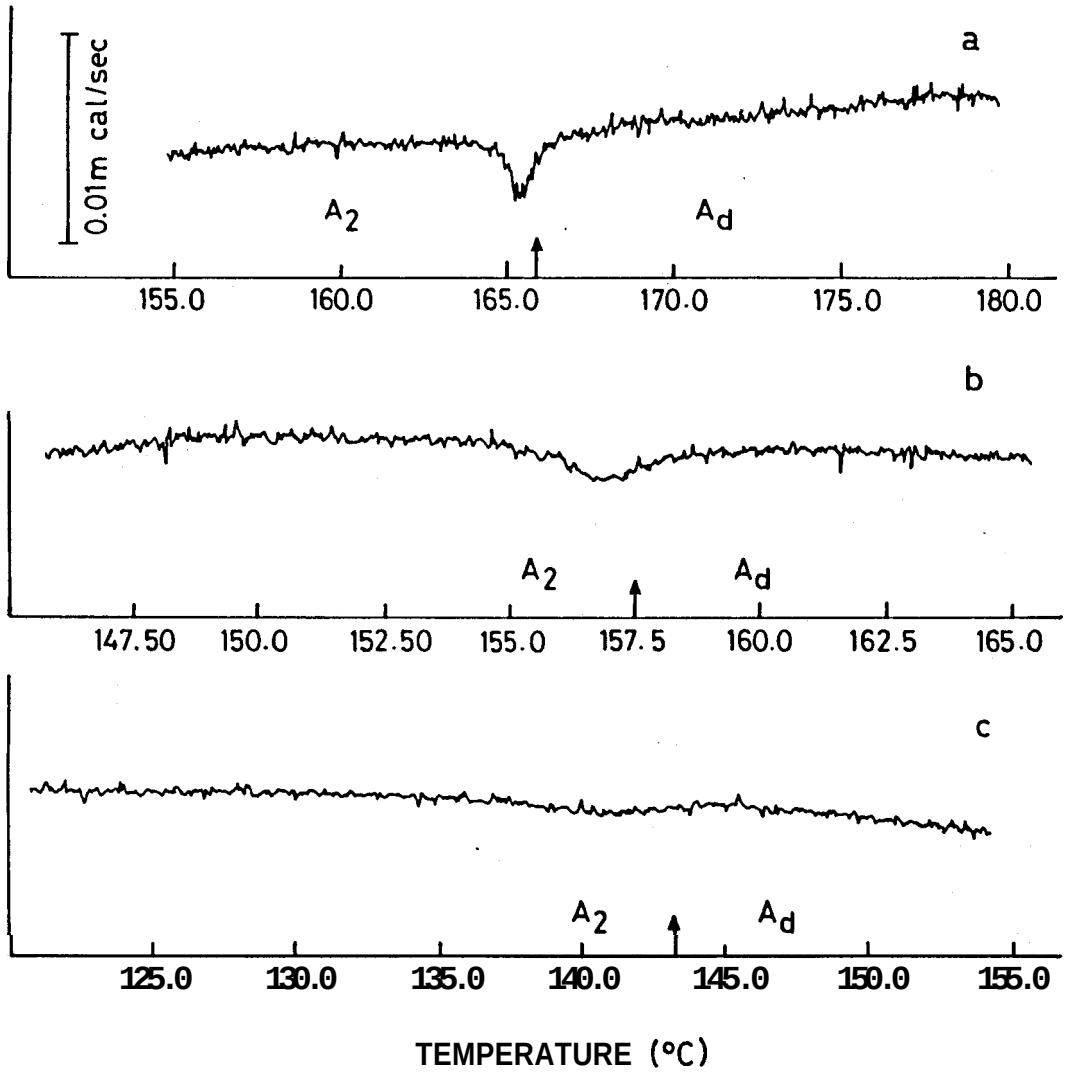

Figure 3.24a,b,c

DSC scans for different concentiations of 8OCB: (a) 6.30%, (b) 12%, and (c) 20% exhibiting only the A_d-A_2 transitions. The transition temperatures aie shown by arrows. A44 the runs were taken at 0.5°C/min. cooling iate.

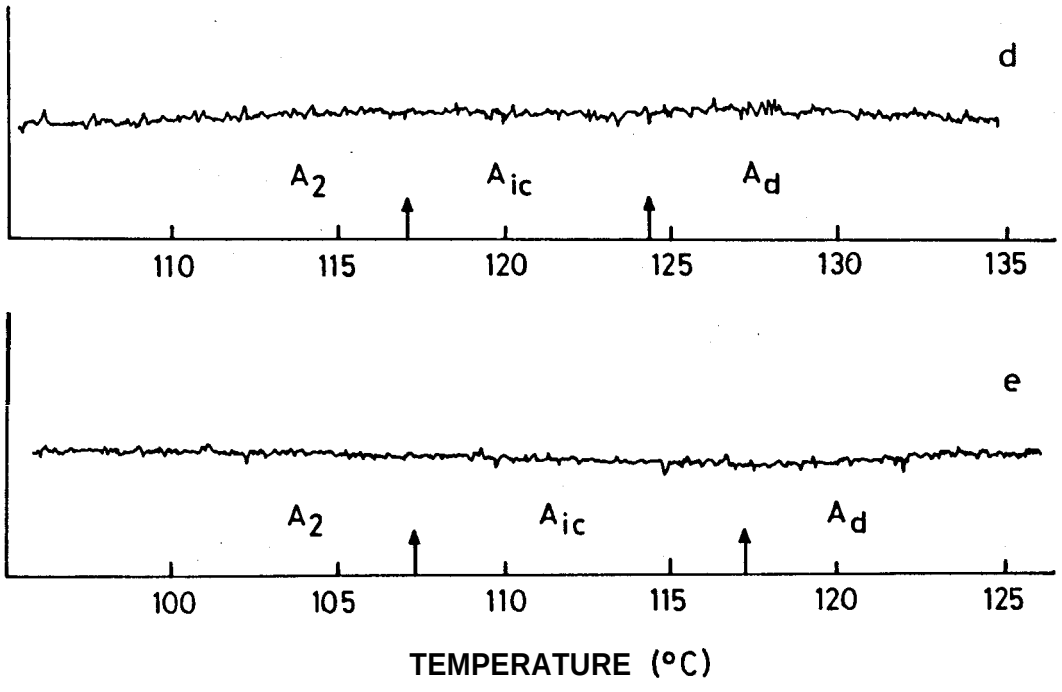

Figure 3.24d,e

DSC scans for different concentrations of 8OCB: (d) 31% and (e) 35.20% exhibiting A_d, A_{ic}, and A_2 phases. The transition temperatures are shown by arrows. All the runs weze taken at 0.5°C/min. cooling rate.

for at least an hour so that a good base line was obtained. It is interesting to observe that the $A_d - A_2$ transition shows a rapid decrease in the strength of the signal with increasing 80CB concentration (see Fig. 3.24a-e). In fact at X = 20% which is only a few per cent away from the concentration at which A_{ic} makes its appearance, the transition is seen as a barely perceptible baseline change. It should be emphasized that in the region where A_{ic} phase exists (see Fig. 3.24d-e), no signals were observed corresponding to the $A_d - A_{ic}$ and $A_{ic} - A_2$ transitions.

3.5 COMPARISON OF THE EXPERIMENTAL PHASE DIAGRAM EXHIBITING THE A_{ic} PHASE WITH A RECENT THEORETICAL DIAGRAM

It may be recalled that Prost and Barois[25] while discussing the phenomenological model, have pointed out that in the weak coupling case, the fourth order terms have to be considered for the minimization of the free energy. This has in fact been done by Barois[37] who has expressed the free energy by including the fourth order terms also. He has shown that the phase diagram represented in the temperature-incommensurability (t-z) plane is fully compatible with our experimental diagram. We shall consider Barois extension of the model in some detail.

As discussed earlier, the uniaxial frustrated smectic phases can be described by two one-dimensionally modulated order parameters, viz., the density modulation described by $\rho(r)$ and the dipolar order parameter $\Phi(r)$ which describes the long range head-to-tail

correlation of the polar molecules along the director :

$$\phi(r) = Re[\psi_1(r)] = Re[|\psi_1| \exp(iq_P z)]$$

$$\rho(r) = Re[|\psi_2|(r)] = Re[|\psi_2| \exp.(iq_\rho Z)]$$

where q_P and q_P denote the wavevectors for the polarization wave and density wave respectively, ψ_1 and ψ_2 being the corresponding fields. In terms of these fields the Landau free energy described in the earlier section reduces to :

$$F = \int \left\{ \frac{1}{2}[A_1 + C_1(\nabla^2 + K_1^2)^2]\phi^2 + \frac{1}{2}[A_2 + C_2(\nabla^2 + K_2^2)]\rho^2 + D_{12}Re(\phi^2\rho) + \frac{B_1}{4}\phi^4 + \frac{B_2}{4}\rho^4 + \frac{B_{12}}{2}\rho^2\phi^2 \right\} dv$$

where $A_1 = a_1(T - T_1)$ and $A_2 = a_2(T - T_2)$, T_1 and T_2 being the non-interacting mean field transition temperatures of $\psi_1(r)$ and $\psi_2(r)$. In this representation, the incommensurate (A_{ic}) phase is defined by $|\psi_1| \neq 0$, $|\psi_2| \neq 0$ and $q_P \neq 2q_P$. It follows from the incommensurability of q_ρ and q_P that the third order coupling term $- D_{12} Re(\phi^2 \rho)$ oscillates along the Z-axis and hence averges to zero in the A_{ic} phase.

Minimisation with respect to the wavevectors and appropriate rescaling of variables[38] lead to the following free energy which is analogous to that which describes the bicritical-tetracritical problem.[39]

$$f(S_{Ai}) = y_1 x_1^2 + (1 + \delta u1)\, x_1^4 + y_2 x_2^2 + (1 + \delta u_2)\, x_2^4 + 2x_1^2 x_2^2 \quad (6)$$

with

$$x_1 = \frac{B_{12}}{8D_{12}} (C_1/C_2)^{1/2} |\psi_1|, \qquad (1+\delta B_1) = (16B_1C_2/B_{12}C_1)$$

and

$$x_2 = \frac{B_{12}}{2D_{12}} |\psi_2| \qquad , \qquad (1 + \delta B_2) = (B_2C_1/16B_{12}C_2)$$

Barois has evaluated phase diagrams by choosing $\delta u1 = 9$ and $\delta u2 = 0$ for different incommensurability parameters (Z) defined by

$$Z = (2B_{12}D_1)^{1/2} (K_1^2 - \frac{K_2^2}{4}) 1/D_{12}$$

K_1 and K_2 are the **minimised** values of q_P and q_ρ respectively.

Barois observed that the topological features of the theoretical phase diagram in the (y_1, y_2) plane at constant Z does not resemble the experimental DB70CN-80CB diagram, even with rotated axes. This is not surprising since it is clear that the (y_1, y_2) representation at constant incommensurability parameter Z is not appropriate to describe the DB70CN - 80CB system - the ratio of the two lengths, i.e., ℓ'/ℓ, varies strongly from DB70CN ($\frac{\ell'}{\ell} \sim 1.9$) to 80CB ($\frac{\ell'}{\ell} - 1.4$). Therefore the incommensurability parameter Z should increase significantly from DB70CN to 80CB. To circumvent this problem, Barois represented the theoretical phase diagram in the

(t,Z) plane so that Z is now related to the concentration as depicted in the experimental T-X diagram. The resultant phase diagram is shown in Fig. 3.25. It is clear that the topology of this diagram is in very good agreement with the experimental DB70CN - 80CB diagram (see Fig. 3.13).

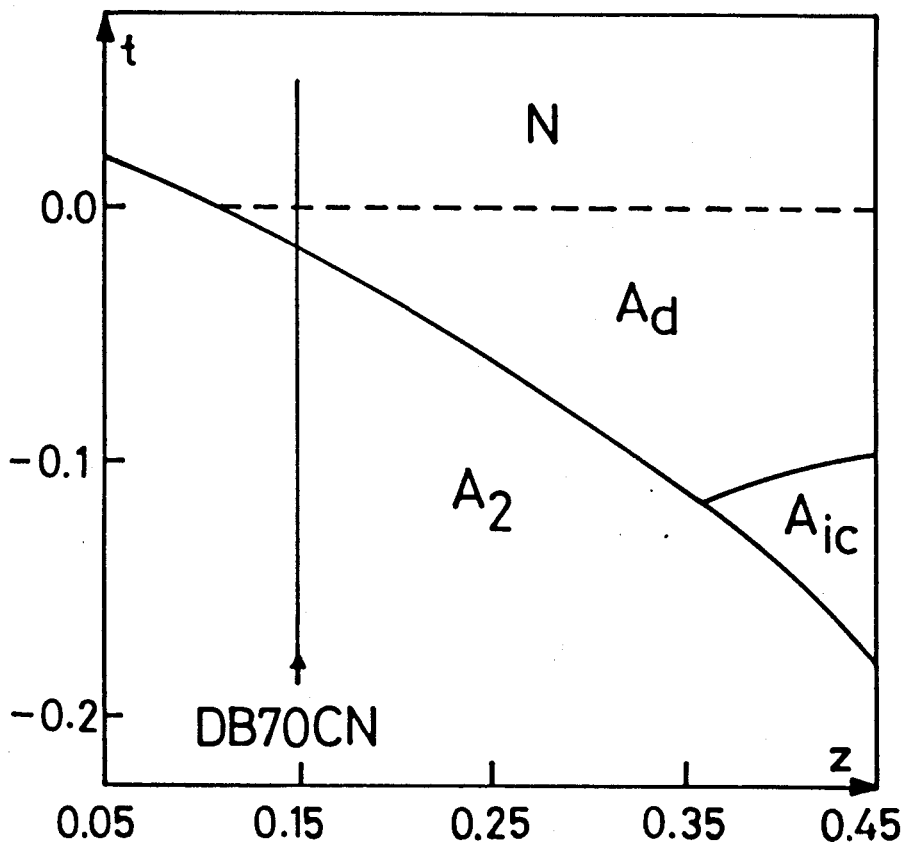

Figure 3.25

Theoretical plot of temperature (t) vs. incommensurability parameter (Z) taken from Ref. 37.

APPENDIX

After the work described in this chapter was* completed, high resolution X-ray studies[4,] on DB7OCN were reported. These studies showed that there is in fact no $A_d - A_2$ transition in DB7OCN, but the A_2 phase evolves continuously from A_d phase. Although these results do not affect any of our conclusions regarding the A_{ic} phase, it does change the over-all situation concerning the phase diagram. We shall enumerate this point further.

Since DB7OCN itself does not exhibit the $A_d - A_2$ transition, the $A_d - A_2$ line shown in Fig. 3.13 is therefore a spurious one. In view of this, the phase diagram now gets modified so that the A_{ic} phase can be considered as being surrounded' by A_d & A_2 phases, A_2 evolving continuously from A_d without a phase transition. For $X > 24\%$, A_{ic} intervenes between A_d and A_2 phases. Interestingly, such a phase diagram has in fact been predicted theoretically41 (see Fig. 3.26).

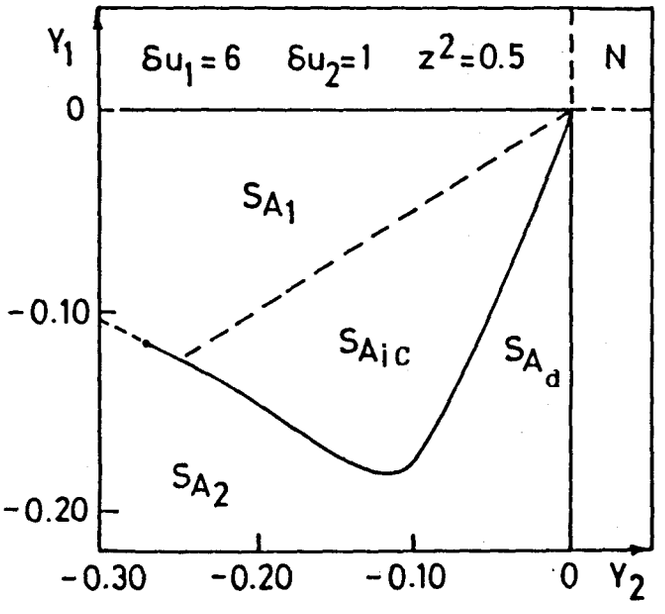

Figure 3.26

Theoretical phabe diagram drawing the exirtence of A_{ic} phaoe surrounded by A_d and A_2 phases. Beyond the region of exirtence of A_{ic}, A_2 is been to evolve continuously from A_d without a phabe transition. (From Ref. 41).

REFERENCES

1 For an introduction to smectic liquid crystals, see S.Chandrasekhar, "Liquid Crystals", Cambridge University Press, Cambridge (1977); see also P. C. de Cennes, "The Physics of Liquid Crystals", (Clarendon Press, Oxford, 1974)

2 A.de Vries, Mol. Cryst. Liq. Cryst., 11, 361 (1970); M.Lambert and A.M.Levelut, C. R. Acad. Sci., Paris 272B, 1018 (1971); S.Diele, P.Brand and H.Sackmann, Mol. Cryst. Liq. Cryst., 16, 105 (1972)

3 W.L.McMillan, Phys. Rev. A, 4, 1238 (1971); P. G. de Gennes, Solid State Commun., 10, 753 (1972)

4 R.Schaetzing and J.D.Litster, "Advances in Liquid Crystals", Vol. 4, Ed. G.H.Brown (Academic Press, 1979), p. 147.

5 J. Als-Nielsen, J.D.Litster, R.J.Birgeneau, M.Kaplan, C.R. Safinya, A.Lindegaard-Anderson and S. Mathiesen, Phys. Rev. B, 22, 312 (1980)

6 J.D.Litster, C.W.Garland, K.J.Lushington and R.Schaetzing, Mol. Cryst. Liq. Cryst., 63, 145 (1981); J.D.Litster, Phil. Trans. Royal Soc. London, A309, 145 (1983)

7 L.D.Landau and R.M.Lifshitz, Statistical Physics, Chap. XIII (Pergamon, 1958)

8 J. Als-Nielsen, R.J.Birgeneau, M. Kaplan, J. D. Litster and C.R.Safinya, Phys. Rev. Lett., 39, 1668 (1977)

9 N.V.Madhusudana and S.Chandrasekhar, Proc. Int. Liq. Cryst. Conf., Bangalore, Pramana, Suppl. 1, 57 (1973)

10 B.R.Ratna and R.Shashidhar, Mol. Cryst. Liq. Cryst., 42, 113 (1977)

11 A.J.Leadbetter, R.M.Richardson and C.N.Colling, J. de Phys., 36, C1-37 (1975)

12 A.J.Leadbetter, J.C.Frost, J.P.Gaughan, G.W.Gray and A.Mosley, J. de Phys., 40, 375 (1979)

13 J.E.Lydon and C.J.Coakley, J. de Phys., 36, C1-45 (1975)

14 P.E.Cladis, Phys. Rev. Lett., 35, 48 (1.975); P.E.Cladis, R.K.Bogardus, W.B.Daniels and G.N.Taylor, Phys. Rev. Lett., **39**, 720 (1977)

15 F.Hardouin, G.Sigaud, M.F.Achard and H.Gasparoux, Phys. Lett., **71A**, 347 (1979); N.V.Madhusudana, B.K.Sadashiva and K.P.L.Moodithaya, Curr. Sci., 48, 613 (1979)

16 For a recent review on smectic A polymorphism, see F.Hardouin, A. M. Levelut, M.F.Achard and G.Sigaud, J. Chim. Phys., 80, 53 (1983)

17 G.Sigaud, F.Hardouin, M.F.Achard and H.Gasparoux, J. de Phys., 40, C3-356 (1979)

18 F.Hardouin, A.M.Levelut, J.J.Benattar and G.Sigaud, Sol. State Commun., 33, 337 (1980)

19 G.Sigaud, F.Hardouin, M.F.Achard and A.M.Levelut, J. de Phys., 42, 107 (1981)

20 A.M.Levelut, J. de Phys. Lett., 45, L-603 (1984)

21 G.Sigaud, F.Hardouin and M.F.Achard, Phys. Rev. A, 31, 547 (1985)

22 G.Sigaud, M.F.Achard and F.Hardouin, J. de Phys. Lett., 46, L-825 (1985)

23 F.Hardouin, Nguyen Huu Tinh, M.F.Achard and A.M.Levelut, J. de Phys. Lett., 43, L-327 (1982); C. R. Acad. Sci. Paris, 284, 355 (1982).

24 J. Prost, Proc. Conf. on Liquid Crystals of One- and Two-Dimensional Order, Eds. W.Helfrich and G.Heppke (Berlin, Springer-Verlag, 1980), p. 125.

25 J. Prost and P. Barois, J. Chim. Phys., 80, 65 (1983)

26 R.B.Meyer and T.C.Lubensky, Phys. Rev., 1 2307 (1976)

27 F.C.Frank and J. H. Van der Merwe, Proc. Roy. Soc. London, **A198**, 216 (1949); **A200**, 125 (1949)

28 P. G. de Gennes, Sol. State Comm., 6, 163 (1968)

29 P. Barois and J.Prost, Ferroelectrics, 58, 193 (1984)

30 P. Barois, "Problems d'incommensurabiliti dans les cristaux liquides i polaires: smectiques frustre's". Thise de specialite Universitide Bordeaux l, 1981, No. 1748.

31 J.Prost, Advances in Physics, 33, 1 (1984)

32 G.J.Brownsey and A.J.Leadbetter, Phys. Rev. Lett., 44, 1608 (1980)

33 C.S.Rosenblatt, R. Pindak, N.A.Clark and R.B.Meyer, J. de Phys., 38, 1105 (1977)

34 F.Hardouin, M.F.Achard, C. Destrade and Nguyen Huu Tinh, J. de Phys., 45, 765 (1984)

35 See, e.g., C.S.Barrett and T.B.Massalski, "Structure of Metals",, McGraw Hill Series Material Science and Engg. (1966)

36 B.D.Cullity, "Elements of X-ray Diffraction" (Addison-Wesley Pub. Co. Inc., 1956)

37 P. Barois, Phys. Rev. A, 33, 3632 (1986)

38 P.Barois, J. Prost and T.C.Lubensky, J. de Phys., 46, 391 (1985)

39 J.M.Kosterlitz, D.R.Nelson and M.E.Fisher, Phys. Rev. B, 13, 412 (1976)

40 S.Krishna Prasad, R.Shashidhar, B.R.Ratna, G.Heppke and S.Pfeiffer, Liq. Cryst., 2, 111 (1987)

41 P. Barois, "These l'Universite de Bordeaux IN d'Ordre 875, "Effects de frustration dans les systems a ordre unidimensional appliction aure smectiques polaires", Ph. D. Thesis, Bordeaux 1987.